Quantitative firing pattern phenotyping of hippocampal neuron types

Abbreviated title: Firing patterns of hippocampal neuron types

Alexander O. Komendantov, Siva Venkadesh, Christopher L. Rees, Diek W. Wheeler, David J. Hamilton, Giorgio A. Ascoli

Krasnow Institute for Advanced Study, George Mason University, 4400 University Drive, MS 2A1, Fairfax, Virginia 2230

Corresponding authors: Alexander O. Komendantov (akomenda@gmu.edu), Giorgio A. Ascoli (ascoli@gmu.edu)***,*** Krasnow Institute for Advanced Study, George Mason University, 4400 University Drive, MS 2A1, Fairfax, Virginia 2230

Number of pages: 72

Number of figures: 8; number of tables: 5 (including 1 color table and 1 box)

Number of multimedia: 0; number of 3D models: 0

Number of words in Abstract: 250; Number of words in Introduction: 648

Number of words in Discussion: 1452

Acknowledgements

This work was supported by grants from the National Institutes of Health (NS39600) and the National Science Foundation (IIS-1302256). We thank Charise M. White and Keivan Moradi for useful discussions and Amar Gawade for help with the web portal. The authors declare no competing financial interests.

Abstract

Systematically organizing the anatomical, molecular, and physiological properties of cortical neurons is important for understanding their computational functions. Hippocampome.org defines 122 neuron types in the rodent hippocampal formation (dentate gyrus, CA3, CA2, CA1, subiculum, and entorhinal cortex) based on their somatic, axonal, and dendritic locations, putative excitatory/inhibitory outputs, molecular marker expression, and biophysical properties such as time constant and input resistance. Here we augment the electrophysiological data of this knowledge base by collecting, quantifying, and analyzing the firing responses to depolarizing current injections for every hippocampal neuron type from available published experiments. We designed and implemented objective protocols to classify firing patterns based on both transient and steady-state activity. Specifically, we identified 5 transients (delay, adapting spiking, rapidly adapting spiking, transient stuttering, and transient slow-wave bursting) and 4 steady states (non-adapting spiking, persistent stuttering, persistent slow-wave bursting, and silence). By characterizing the set of all firing responses reported for hippocampal neurons, this automated classification approach revealed 9 unique families of firing pattern phenotypes while distinguishing potential new neuronal subtypes. Several novel statistical associations also emerged between firing responses and other electrophysiological properties, morphological features, and molecular marker expression. The firing pattern parameters, complete experimental conditions (including solution and stimulus details), digitized spike times, exact reference to the original empirical evidence, and analysis scripts are released open-source through Hippocampome.org for all neuron types, greatly enhancing the existing search and

43 browse capabilities. This information, collated online in human- and machine-accessible
44 form, will help design and interpret both experiments and hippocampal model simulations.

45

46 **Significance Statement**

47 Comprehensive characterization of nerve cells is essential for understanding
48 signal processing in biological neuronal networks. Firing patterns are important
49 identification characteristics of neurons and play crucial roles in information coding in
50 neural systems. Building upon the comprehensive knowledge base Hippocampome.org,
51 we developed and implemented automated protocols to classify all known firing
52 responses exhibited by each neuron type of the rodent hippocampus based on analysis
53 of transient and steady-state activity. This approach identified the most distinguishing
54 elements of every firing phenotype and revealed previously unnoticed statistical
55 associations of firing responses with other electrophysiological, morphological, and
56 molecular properties. The resulting data, freely released online, constitute a powerful
57 resource for designing and interpreting experiments as well as developing and testing
58 hippocampal models.

59

60

61 **Introduction**

62 Quantitative characterization of neurons is essential for understanding the
63 functions of neuronal networks at different hierarchical levels. The hippocampus provides

an excellent test-bed for this exploration as it is one of the most intensively studied parts of the mammalian brain, and is involved in critical functions including learning (Rudy and Sutherland, 1989, 1995), memory (Eichenbaum et al., 1992; Eichenbaum, 2000, 2017), spatial navigation (Hafting et al. 2005; O'Keefe and Dostrovsky, 1971), and emotional associations (Buchanan, 2007).

Transmission of information between neurons is carried out by sequences of spikes, and firing rates are commonly believed to represent the intensity of input stimuli. Since the first discovery in sensory neurons (Adrian and Zotterman, 1926), this principle was generalized and extended to neurons from different brain regions including the hippocampus (McNaughton et al, 1983). However, it was also found that the firing rate of certain neurons is not constant over time even if the stimulus is permanently applied. One form of such time-dependent responses is spike frequency adaptation, manifested in a decrease of firing rate (Adrian and Zotterman, 1926). Neurons can produce diverse firing patterns in response to similar stimuli due to the inhomogeneity in their intrinsic properties (Connors and Gutnick, 1990). Both firing rates and temporal firing patterns are now recognized to play important roles in neural information coding (Ferster and Spruston, 1995).

In electrophysiological experiments *in vitro*, hippocampal neurons demonstrate a vast diversity of firing patterns in response to depolarizing current injections. These patterns are referred to by many names, including delayed, adapting, accommodating, interrupted spiking, stuttering, and bursting (Canto and Witter 2012a,b; Hemond et al., 2008; Lübke et al, 1998; Mercer et al., 2007; Pawelzik et al., 2002; Tricoire et al., 2011).

Uncertainties and ambiguities in classification and naming of neuronal firing patterns are similar to other widely spread terminological inconsistencies in the neuroscience literature, posing obstacles to effective communication within and across fields (Hamilton et al., 2017).

Recent efforts aimed to develop firing pattern classification for identifying distinct electrical types of cortical neurons (Markram et al., 2004, 2015; Petilla Interneuron Nomenclature Group et al., 2008). Notably, statistical analysis of a large set of electrical features of neocortical interneurons with different firing patterns from a single lab yielded a refinement of the physiological component of the Petilla Nomenclature (Druckmann et al., 2013). However, comparisons across labs and experimental studies are typically limited to qualitative assessments of the illustrated firing traces or subjectively intuitive criteria. Moreover, firing pattern data are seldom unambiguously linked to neuron types independently defined by morphological and molecular criteria.

The Hippocampome.org knowledge base defines neuron types based on the locations of their axons, dendrites, and somata across 26 parcels of the rodent hippocampal formation, putative excitatory/inhibitory output, synaptic selectivity, and major and aligned differences in molecular marker expressions and biophysical properties (Wheeler et al., 2015). Version 1.3 of Hippocampome.org identified 122 neuron types in 6 major areas: 18 in dentate gyrus (DG), 25 in CA3, 5 in CA2, 40 in CA1, 3 in subiculum (SUB), and 31 in entorhinal cortex (EC). The core assumption of this identification scheme is that neurons with qualitatively different axonal or dendritic patterns, or with multiple substantial differences in other dimensions, belong to different types. For the majority of

neuron types, Hippocampome.org reports 10 basic biophysical parameters that numerically characterize passive and spike properties (hippocampome.org/ephys-defs), consistent with other literature-based neuroinformatics efforts (Tripathy et al., 2015).

Here, we developed an objective numerical protocol to automatically classify all published electrophysiological recordings of somatic spiking activity for morphologically identified hippocampal neurons from Hippocampome.org. This process revealed specific firing pattern phenotypes, potential neuronal subtypes, and statistical associations between firing responses and other properties. Inclusion of the classified firing patterns and their quantitative parameters, along with a comprehensive tabulation of the underlying experimental conditions, substantially extends the online search and browse functionalities of Hippocampome.org, providing a wealth of annotated data for quantitative analysis and modeling.

Materials and Methods

Data collection, extraction and digitization. The firing patterns of hippocampal neurons were classified based on their spiking responses to supra-threshold step-current pulses of different amplitude and duration as reported in peer-reviewed publications. Firing pattern parameters were extracted from electronic figures using Plot Digitizer (plotdigitizer.sourceforge.net) for all Hippocampome.org neuron types (Wheeler et al., 2015) for which they were available (90 out of 122). A total of 247 traces were analyzed. We extracted values of first spike latency (i.e. delay), inter-spike intervals (ISIs), and post-firing silence (in ms), as well as slow-wave amplitude (in mV) for burst firing recording.

For firing pattern identification and analysis, ISIs in each recording were normalized to the shortest inter-spike interval (ISI_{min}) within that time series, to allow meaningful comparison.

All analyzed recordings were obtained in normal artificial cerebrospinal fluids (ACSF) from rodents (rats 85%, mice 12%, and guinea pigs 3%) generally described as 'young adults' (ages ranging from 11 to 70 days for rats and from 10 to 56 days for mice). All firing traces considered in this report were recorded in slice preparations; 74% of electrophysiological traces were obtained using whole-cell patch clamp and 26% intracellular recording with sharp microelectrodes. All experimental conditions and solution compositions were extracted and stored with every recording and are available at Hippocampome.org as specified in the "Web portal" section below. Representative examples of ACSF and of solutions for pipette filling are shown in Table 1 and Table 2, respectively.

[Table 1 is near here]

[Table 2 is near here]

Firing pattern classification. Hippocampal neuron types display a variety of firing pattern elements in both their transient and steady state responses to continuous stimulation (Figure 1). Specifically, transients (which we label by dot-notation) can be visually differentiated into delay (D.), adapting spiking (ASP.), rapidly adapting spiking (RASP.), transient stuttering (TSTUT.), and transient slow-wave bursting (TSWB.). Steady states include silence (SLN), non-adapting spiking (NASP), persistent stuttering (PSTUT), and persistent slow-wave bursting (PSWB).

[Figure 1 is near here]

In certain cases, a constant current injection elicits firing patterns consisting of single firing pattern elements (NASP, PSTUT or PSWB). In other cases, complex firing patterns are observed as sequences of two or more firing pattern elements, such as delayed non-adapting spiking (D.NASP), silence preceded by adapting spiking (ASP.SLN), and non-adapting spiking preceded by delayed transient slow-wave bursting (D.TSWB.NASP). Experimental recordings without identifiable steady states were deemed uncompleted firing patterns (e.g. ASP., D.ASP., or RASP.ASP.).

In order to define the firing pattern elements unambiguously, we developed a set of quantitative classification criteria (Table 3). The transient response was classified as delayed (D.) if the latency to the first spike was longer than the sum of the first two inter-spike intervals (ISI_1 and ISI_2). Similarly, post-firing silence (PFS) was considered to be a steady state (SLN) if it exceeded the sum of the last two inter-spike intervals (ISI_{n-1} and ISI_n). In addition, post-firing silence had to last at least twice the longest inter-spike interval (ISI_{max}).

A persistent firing response with relatively equal inter-spike intervals denotes non-adapting spiking (NASP); in contrast, transients with a progressive increase or decrease of ISIs can be classified as adapting or accelerating spiking, respectively. To discriminate among several possible combinations of these firing patterns objectively and reproducibly, we devised a minimum information description criterion by comparing piecewise (segmented) linear regression models of increasing complexity. Specifically, non-adapting spiking (NASP) can be described by a single parameter, namely the

(average) firing rate ($Y=c$). Similarly, fitting normalized inter-spike intervals versus normalized time with a (2-parameter) linear function $Y=aX+b$ (with $a>0$) corresponds to adapting spiking (ASP.). Fitting data with a piecewise linear function

$$Y = \begin{cases} a_1 X + b_1 & if\ X < \dfrac{b_2 - b_1}{a_1 - a_2} \\ a_2 X + b_2 & if\ X \geq \dfrac{b_2 - b_1}{a_1 - a_2} \end{cases}$$

corresponds to adapting-non-adapting spiking (ASP.NASP) when $a_1>0$ and $a_2=0$ (3 parameters), and to adapting-adapting spiking with different adaptation rates (ASP.ASP.) when both $a_1>0$ and $a_2>0$ (4 parameters). We only selected a model with more parameters if the fit relative to a less complex model improved in a statistically significant way. The significance threshold for the differences between one-parameter fitting (NASP) and two-parameter linear-regression fitting (ASP.) was conventionally set at 0.05. Furthermore, in order to avoid identifying very weak adaptations as ASP., a minimum threshold of 0.003 was used for the slope a_1.

[Table 3 is near here]

For each subsequent stage of comparison, we used Bonferroni-corrected *p*-values. Specifically, in order for a pattern with an adapting spiking transient (i.e. ASP.) to be qualified as ASP.NASP, the *p*-value must be less than 0.025. Similarly, the *p*-value for the differences between three-parameter piecewise-linear-regression fitting (ASP.NASP) and four-parameter piecewise-linear-regression fitting (ASP.ASP.) must be less than 0.016. Figure 2 shows examples of fitting spiking activity with linear regression and

193 piecewise linear regression models. If adaptation was only observed in the first two or
194 three ISIs in a longer train of spikes, and if the linear fitting of slope a_1 exceeded 0.2, then
195 this transient was classified as rapidly adapting spiking (RASP.) (see Fig.1; cf. Pawelzik
196 et al., 2002). For accelerating spiking (ACSP.), the linear fitting slope must be negative.

197 [Figure 2 is near here]

198 We defined transient stuttering (TSTUT.) as a short high-frequency (>25 Hz)
199 cluster of action potentials (APs) followed by other distinctive activity. In addition, the first
200 ISI after a TSTUT cluster must be 2.5 times longer than the last ISI of the cluster and 1.5
201 times longer than the next ISI (see Fig. 1; cf. Hamam et al., 2000). Under transient slow-
202 wave bursting activity (TSWB.), a cluster of two or more spikes rides on a slow
203 depolarization wave (>5mV) followed by a strong slow after-hyperpolarization (AHP) (see
204 Fig. 1; cf. Chevaleyre and Siegelbaum 2010). Persistent stuttering (PSTUT) was
205 classified as firing activity with high-frequency clusters of APs separated by silence
206 intervals >5 times longer than the sum of the preceding and following ISIs (see Fig. 1; cf.
207 Fuentealba et al. 2010; Price et al. 2005). Similarly, under persistent slow-wave bursting
208 (PSWB) activity, these clusters of two or more tightly grouped spikes ride on slow
209 depolarizing waves (>5 mV) followed by strong, slow AHPs (Golomb et al. 2006; Bilkey
210 and Schwartzkroin 1990). As exemplified above, the choices of firing pattern identification
211 parameters were consistent with literature reports of experimental results with similar
212 activities.

213 *Algorithm Implementation.* Based on the aforementioned methods, we
214 implemented a firing pattern classification algorithm (Fig. 3) using the values of ISIs,

delay, post-firing silence, and slow-wave amplitude as input data. Firing pattern elements were identified based on calculated characteristics of responses (Table 3). First, it was determined whether the pattern contained a delay (D.), then whether it contained a TSTUT. or TSWB. The remaining ISIs were processed using the described statistical test to identify spike frequency adaptation (ASP., ASP.NASP, ASP.ASP.) by fitting the sequence of intervals with a piecewise linear function. In the case of an incomplete pattern or an insufficient number of ISIs to perform the test, the presence of post firing silence (SLN) was checked. If the test did not identify the pattern containing the adaptation, then the firing pattern was checked for the presence of PSTUT or PSWB, and then for NASP or RASP. If rapid adaptation was detected, the cycle with the statistical test was performed again on the remaining ISIs. The algorithm terminated upon detection of one of the steady states (SLN, NASP, PSTUT, or PSWB).

Software Accessibility. The classification algorithm was initially piloted in Microsoft Excel (Visual Basic) using Solver and the Data Analysis Toolbox (F-test and t-test) to perform piecewise linear fitting and statistical tests. The program was then re-implemented in the Java programming language using the Apache Commons Mathematics Library (commons.apache.org/proper/commons-math). The Java implementation is available open source at github.com/Hippocampome-Org/NeuroSpikePatterns.

[Figure 3 is near here]

Experimental Design and Statistical Analysis. We explored pairwise correlations between all observed firing patterns, firing pattern elements, and 316 properties of

Hippocampome.org neuron types, including: primary neurotransmitter; axonal, dendritic, and somatic locations in the 6 sub-regions and 26 parcels of the hippocampal formation; the projecting (between sub-regions) or local (within sub-regions) nature of axonal and dendritic patterns; axon and dendrite co-presence within any parcel; axonal and dendritic presence in a single layer only (intra-laminar) or in ≥3 layers (trans-laminar); clear positive or negative expression of any molecular markers; high (top third) or low (bottom third) values for biophysical properties (Wheeler et al., 2015); and potential connectivity patterns and super-patterns (Rees et al., 2016). To evaluate the correlations between these categorical properties, we used 2×2 contingency matrices with Barnard's exact test (Barnard, 1947), which provides the greatest statistical power when row and column totals are free to vary (Lydersen et al., 2009). The correlation analysis was implemented in MATLAB (MathWorks, Inc.).

We analyzed numerical electrophysiological data, such as the relationship between the width of an action potential and the minimum ISI using linear regression and histograms. Spike duration was measured as the width at half-maximal amplitude as is most commonly defined (Bean, 2007). Minimum inter-spike intervals (ISI_{min}) were extracted from digitized recordings or directly from tables or textual excerpts of the corresponding papers.

For cluster analysis of weighted categorical firing pattern data, we assigned weights to firing pattern elements according to the formula $W_e=(N-n_e)/N$, where W_e is the weight of the element e, n_e is the number of cell types expressing firing pattern(s) with element e, N is the total number of cell types/subtypes, and e={ASP., D., RASP., NASP,

PSTUT, PSWB, SLN, TSUT., TSWB.}. We employed a two-step cluster analysis using the IBM SPSS Statistics 24 software. Silhouette measures of cohesion and separation greater than 0.5 indicated that the elements were well matched to their own clusters and poorly matched to neighboring clusters, and that the clustering configuration was appropriate.

Statistical data were expressed as mean ± standard deviation.

Web portal and database representation of firing patterns and experimental conditions. Hippocampome.org provides access to morphological, molecular, electrophysiological, and connectivity information for 122 neuron types. The firing pattern data newly added and made freely available for download with this work include recording illustrations, the duration and amplitude of stimulation, digitized ISIs and firing pattern parameters (as comma-separated-value files), the complete solution compositions of the ACSF and of the micropipettes or patch pipettes, and the result of the firing pattern classification algorithm detailed above. Additional metadata is collected and displayed for all electrophysiological evidence in Hippocampome.org including the animal species (rat vs. mouse) and other details regarding the subject (inbred strain, age, sex, and weight, if reported), slice thickness and orientation, recording methods (intracellular microelectrode or variations of patch clamp), and temperature.

The implementation of Hippocampome.org supports the model-view-control software design. The model component defines the database interface and is provided solely by server-side code. The view component rendering the web pages and the control code implementing the decision logic are both served up by the server, but are run in the

user's browser. The underlying relational database ensures flexibility in establishing relations between data records.

Hippocampome.org is deployed on a CentOS 5.11 server running Apache 2.2.22 and runs on current versions of several web browsers (Mozilla Firefox, Google Chrome, Apple Safari, and Microsoft Internet Explorer). Knowledge base content is served up to the PHP 5.3.27 website from a MySQL 5.1.73 database. Django 1.7.1 and Python 3.4.2 provide database ingest capability of comma separated value annotation files derived from human-interpreted peer-reviewed literature. Hippocampome.org code is available at github.com/Hippocampome-Org.

Results

From firing patterns to firing pattern phenotypes

Version 1.3 of Hippocampome.org contains suitable electrophysiological recordings for 90 of the 122 morphologically identified neuron types. Applying the firing pattern identification algorithm to these digitized data resulted in the detection of 23 different firing patterns. A given neuron type may demonstrate distinct firing patterns in response to different stimuli or conditions. The set of firing patterns exhibited by a given neuron type forms its firing pattern phenotype.

The simplest case consists of those neuron types that systematically demonstrate the same firing pattern independent of experimental conditions or stimulation intensity. These neuron types may still display quantitatively different responses to stimuli of

various amplitudes (typically increasing their firing frequency upon increasing stimulation), but their qualitative firing patterns remain the same. We identified 37 such "individual/simple-behavior types" in Hippocampome.org, as exemplified by DG Basket cells with their NASP phenotype (Savanthrapadian et al., 2014).

In contrast to the above scenario, certain neuron types exhibit qualitatively distinct firing patterns in response to different amplitudes of stimulation. We identified 21 such "multi-behavior" types; for instance, CA1 Neurogliaform cells (Price et al., 2005; Tricoire et al., 2011) display delayed firing, adapting spiking, and persistent stuttering at different stimulus intensities. The firing phenotype of these interneurons thus consists of the combination of all three firing patterns.

In a different set of cases, subsets of neurons from the same morphologically identified type display distinct firing patterns under the same experimental conditions (typically from the same study) in response to identical stimulation. These neuron types can thus be divided into electrophysiological subtypes. For example, of the CA3 Spiny Lucidum interneurons, some are adapting spikers whereas others are persistent stutterers (Szabadics and Soltesz, 2009). In certain neuron types, one or more of the subtypes could also display multiple behaviors at different stimulation intensities. For instance, a subset of entorhinal Layer III Pyramidal neurons consists of non-adapting spikers and another subset switches from ASP.NASP at rheobase to RASP.ASP. at higher stimuli (Canto and Witter, 2012b). Of the 90 neuron types with firing patterns in Hippocampome.org, 22 could be divided into 52 electrophysiological subtypes. Notably, these included the principal neurons of most sub-regions of the hippocampal formation:

CA3, CA1, and subiculum Pyramidal cells, entorhinal Spiny Stellate cells, but also several GABAergic interneurons such as Total Molecular Layer (TML) cells (Mott et al, 1997). Specifically, 8 neuron types yielded 18 subtypes exclusively demonstrating single behaviors; for 11 neuron types, at least one of the subtypes exhibited multi-behaviors, resulting in 13 multi-behavior subtypes and 13 additional single-behavior subtypes.

This meta-analysis is complicated by the variety of experimental conditions used in the published literature from which the electrophysiological data were extracted. Several differences in materials and methods could affect firing patterns above and beyond common species (rats vs. mice) or recording (patch clamp vs. microelectrode). For example, 30% of experimental traces were recorded from transverse slices, 24% from horizontal, 8% coronal, 29% mixed (e.g. “horizontal or semicoronal”), and 9% other directions (e.g. custom angles). Furthermore, pipettes were filled with potassium gluconate in 69% of cases, with potassium methylsulfate in 22%, and with potassium acetate in 9% (see e.g. Table 2). While these different experimental conditions can affect membrane biophysics substantially (Tebaykin et al., 2018) and often quantitatively influence neuronal firing (e.g. changing the spiking frequency), occasionally they can also cause a qualitative switch between distinct firing patterns. A striking case is that of rat DG Granule cells, which have demonstrated transient slow-wave burst followed by silence in whole-cell recordings of horizontal slices from Sprague-Dawley animals (Williams et al., 2007); delayed non-adapting spiking in whole-cell recording of transverse slices from Wistar animals (Lübke et al., 1998); or adapting spiking in intracellular recording of horizontal slices from Wistar animals (Han et al., 1993). Because the different firing patterns could be caused by the differences in experimental methods, we annotate a

possible "condition-dependence," but cannot conclusively categorize these cells as multi-behavior or subtypes. Most of the condition-dependent behaviors could be attributed at least in part to the occasional use of microelectrode instead of patch-clamp (now considered the preferred recording method) or the animal species as in the case of CA1 Horizontal Basket cells which display adapting and non-adapting firing in rats and mice, respectively (Zemankovics et al, 2010; Tricoire et al, 2011).

Condition dependence can alter the firing patterns not only in cell types with single behaviors, such as MOPP cells (Han et al., 1993; Armstrong et al., 2011), but also in multi-behavior neuron types, such as CA1 Axo-Axonic cells (Buhl et al., 1994; Pawelzik et al., 2002). These cases account for 6 and 4 Hippocampome.org neuron types, respectively. Lastly, condition dependence may also be found in specific electrophysiological subtypes, whether they display single behaviors, such as CA1 Pyramidal neurons (Chevaleyre and Siegelbaum, 2010; Zemankovics et al, 2010; Kirson and Yaari, 2000; Staff et al., 2000) or multi-behavior, such as entorhinal Layer V Deep Pyramidal neurons (Canto and Witter, 2012; Hamam et al., 2000; Hamam et al., 2002). These cases respectively account for 2 and 1 Hippocampome.org neuron types, in turn giving rise to 6 condition-dependent subtypes with single behaviors and 2 condition-dependent subtypes with multi-behavior.

Figure 4 presents the full firing pattern phenotypes of all 90 Hippocampome.org neurons with available data in form of separate matrices for the 68 individual neuron types (Fig. 4A) and the 52 subtypes divided from the remaining 22 types (Fig. 4B). In both cases the simple behaviors constitute larger proportions than multi-behavior with condition

dependence only reported for a minority of types and subtypes (Fig. 4C). Across these neuron types/subtypes, 44 distinct phenotypes can be identified as unique combinations of firing patterns, excluding those that differ from others only by the absence of a detectable stable state in one of the firing patterns (like ASP. versus ASP.NASP or ASP.SLN). An interactive online version of these matrices is available at hippocampome.org/firing_patterns.

[Figure 4 is near here]

Dissecting firing patterns into firing pattern elements across neuron types

Firing patterns and firing pattern elements are also diverse with respect to their relative frequency of occurrence among hippocampal neuron types. Firing patterns can be grouped based on the number of elements comprising them, namely single (e.g., NASP or PSTUT), double (e.g. ASP.NASP or TSWB.SLN), and triple (D.RASP.NASP and D.TSWB.NASP) or based on whether they are completed (ASP.NASP, TSWB.SLN) or uncompleted, as in ASP., RASP.ASP., and TSTUT.ASP. (Fig. 5A). Of the nine firing pattern elements, the most frequent are ASP and NASP, while the least common are TSTUT, TSWB, and PSWB (Fig. 5B). Notably, accelerated spiking (ACSP) has not been reported in the rodent hippocampus although it is commonly observed in other neural systems, such as turtle ventral horn interneurons (Smith and Perrier 2006) and motoneurons (Leroy et al. 2014).

The relationships between sets of firing pattern elements observed in hippocampal neuron types can be summarized in a Venn diagram with firing pattern elements represented as ellipses and the intersections thereof corresponding to complex firing patterns (Fig. 5C). This analysis highlights the following features: the four main firing transients (ASP., RASP., TSTUT., TSWB.) often end either with NASP or with SLN; ASP. is often preceded by RASP. and occasionally by TSTUT.; interrupted steady-state firings (PSTUT and PSWB) stand out as a separate group; and delay (D.) most often precedes NASP.

[Figure 5 is near here]

Our classification of firing pattern elements implies the possibility of three completed single-element firing patterns (NASP, PSTUT, PSWB) and 19 completed double-element firing patterns consisting of one of four steady states (SLN, NASP, PSTUT, PSWB) preceded by one of five transients (D, ASP, RASP, TSTUT, TSWB), with exclusion of the "empty" combination D.SLN. Also, four double-transients are possible after an initial delay, resulting in an additional 16 triple-element firing patterns. Only 15 of these possible 38 completed firing patterns were discovered in literature data for morphologically identified hippocampal neuron types (Table 4). Three additional firing patterns were found in other neurons: D.PSWB has been shown in the cultured *rutabaga* mutant giant neuron of *Drosophila* (Zhao and Wu 1997), D.ASP.SLN in the neuron of the external lateral subnucleus of the lateral parabrachial nucleus (Hayward and Felder 1999), and D.TSTUT.SLN in the striatal fast-spiking neuron (Sciamanna and Wilson 2011). We deemed 16 firing patterns as "not found but possible" (white shading and black text in

Table 4) and 4 firing patterns as “improbable” (white shading and gray text). In particular, we consider combination of stuttering and slow-wave bursting (TSWB.PSTUT or TSTUT.PSWB) as unlikely to occur under physiological conditions from a dynamical viewpoint due to incompatible underlying mechanisms. Slow-wave bursting is provided by a slow negative feedback which terminates the burst of action potential evoking slow AHP. Such feedback could be produced by different ionic mechanisms, but it is most typically based on intracellular Ca^{2+} dynamics and Ca^{2+}-activated K^+ current (Golomb et al. 2006; Xu and Clancy 2008) or muscarinic-sensitive K^+ current (Golomb et al. 2006). Slow-wave bursting could be “square-wave bursting”, with one slow process, or “parabolic bursting”, with two (positive and negative feedback) slow processes (Rinzel and Ermentrout 1998). In contrast, stuttering activity is associated with “elliptic bursting” (Golomb et al. 2007), where the silent phase is characterized by dumping and growing fast (spiking) oscillations as the trajectory slowly drift through bifurcation of the fast subsystem (Rinzel and Ermentrout 1998). Suggested mechanism for stuttering in fast spiking interneurons includes Na^+ “window” current that induces high frequency tonic firing, and slowly inactivating K^+ current through KV1 channels (Golomb et al. 2007).

[Table 4 is near here]

Classification and distribution of firing pattern phenotypes

In order to classify the 44 unique firing pattern phenotypes observed in the hippocampal formation, we weighted the constituent firing pattern elements according to the frequency of occurrence among 120 neuron types and electrophysiological subtypes (see *Materials*

433 *and Methods*). As a result, infrequent firing pattern elements (PSWB, TSTUT and TSWB)
434 received high weights (0.99, 0.95 and 0.93, respectively), very frequent elements (ASP
435 and NASP) were assigned low weights (0.42 and 0.41), and common elements (D, RASP,
436 PSTUT and SLN) obtained intermediate weights (0.90, 0.80, 0.88 and 0.87). Two-step
437 cluster analysis identified ten firing pattern families as leaves of a seven-level hierarchical
438 binary tree (Fig. 6A). At the highest level, hippocampal neuron types and subtypes are
439 divided into two major groups: those with spiking phenotypes (78%) and those with
440 interrupted firing phenotypes (22%). The latter are separated into bursting (6%) and
441 stuttering (16%), and each of these is subdivided into persistent and non-persistent
442 families. A first group of the neuron types with spiking phenotypes is distinguished based
443 on delay (9% of cell types). The remaining neuron types split into adapting (54%) and
444 non-adapting phenotypes (15%). The adapting group consists of neuron types with
445 rapidly adapting phenotypes (18%) and normally adapting (36%) phenotypes. Among the
446 normally adapting group, the following phenotypes can be distinguished: discontinuous
447 adapting spiking (6%) with ASP.SLN pattern, adapting-non-adapting spiking (15%) with
448 ASP.NASP patterns, and a last “spurious” phenotype of uncompleted adapting spiking
449 (15%) with ASP. pattern only, for which the steady state (SLN or NASP) was not
450 determined. This division of the adapting spiking groups reflects differences in adaptation
451 rates, duration, and subsequent steady states.

452 This analysis also highlights the most distinguishing firing pattern elements of each
453 family (Fig. 6B). In particular, D. is the defining element for delayed spiking, PSTUT for
454 persistent stuttering, ASP. and SLN for discontinuous adapting spiking. Each of the four
455 major elements of interrupted firing patterns (PSWB, PSTUT, TSWB. and TSTUT.) is

456 observed in a single firing pattern phenotype (persistent bursting, non-persistent bursting,
457 persistent stuttering, and non-persistent stuttering, respectively). Other firing pattern
458 elements (D., RASP., ASP., NASP, and SLN) appear in several firing pattern phenotypes.
459 The proportions of non-defining firing pattern elements range from 5% to 83%.

460 The families of firing pattern phenotypes are differentially distributed within the set
461 of 120 neuron types/subtypes (Fig. 6C). Certain phenotype families are associated with
462 excitatory neuron types, either exclusively (e.g. persistent bursting and non-persistent
463 bursting) or predominantly (non-persistent stuttering, rapidly adapting, and adapting-non-
464 adapting spiking). Conversely, persistent stuttering, delayed spiking, non-adapting
465 spiking and simple adapting spiking are phenotypes composed largely by inhibitory
466 neuron types. The discontinuous adapting spiking phenotype has relatively balanced
467 proportions of excitatory and inhibitory neuron types.

468 The firing pattern phenotypes also have different distributions among the sub-
469 regions of the hippocampal formation (Fig. 6D). Among CA1 neuron types, the persistent
470 stuttering (16%), non-adapting (24%), simple adapting (16%), and rapidly adapting
471 spiking (13%) phenotypes are more common than other phenotypes; in DG, the most
472 expressed phenotypes are delayed (20%), rapidly adapting (20%), and simple adapting
473 spiking (15%); in EC, ASP-NASP (61%), discontinuous ASP. (11%), RASP. (28%), and
474 NASP (19%) occur more often than other phenotypes.

475 [Figure 6 is near here]

476

Usage of information from Hippocampome.org

Searching and Browsing. The addition of firing pattern data to Hippocampome.org extends opportunities for broad-scope analytics and quick-use checks of neuron types. Similar to morphological, molecular, and biophysical information, firing patterns and their parameters can be browsed online with the interactive versions of the matrices presented in Figure 4 (hippocampome.org/firing_patterns), along with an accompanying matrix to browse the stimulation parameters (duration and intensity) and the firing pattern parameters (delay, number of inter-spike intervals, etc.).

Moreover, all classification and analysis results reported here can be searched with queries containing AND & OR Boolean logic using an intuitive graphical user interface (see Hippocampome.org → Search → Neuron Type). The integration within the existing comprehensive knowledge base enables any combination of both qualitative (e.g. PSTUT) and quantitative (e.g. $\frac{ISI_i^{\max}}{ISI_{i+1}} > 10$) firing pattern properties with molecular (e.g. calbindin-negative), morphological (e.g. axons in CA1 pyramidal layer), and biophysical (e.g. action potential width < 1 ms) filters (Fig. 7). For example, of 14 neuron types with persistent stuttering, in 5 the maximum inter-spike interval is at least an order of magnitude longer than the subsequent spike. When adding the other three selected criteria, the compound search leads to a single hit: CA1 Axo-axonic neurons (Fig. 7A). Clicking on this result leads to the interactive neuron page (Fig. 7B) where all information associated with a given neuron type is logically organized, including synonyms, morphology, biophysical parameters, molecular markers, synaptic connectivity, and firing patterns. Every property on the neuron pages and browse matrices, including firing

patterns and their parameters, links to a specific evidence page that lists all supporting bibliographic citations, complete with extracted quotes and figures (Fig. 7C). The evidence page also contains a table with all corresponding firing pattern parameters (Fig. 7D), experimental details including information about animals (Fig. 7E), preparations (Fig. 7F), recording method and intra-pipette solution (Fig. 7G), ACSF (Fig. 7H), and a downloadable file of inter-spike intervals (Fig. 7I).

[Figure 7 is near here]

The portal also reports, when available, the original firing pattern name descriptions used by the authors of the referenced publication (Hippocampome.org → Search → Original Firing Pattern).

Statistical analysis of categorical data. Firing pattern information more than doubles the Hippocampome.org knowledge base capacity to over 27,000 pieces of knowledge, that is, associations between neuron types and their properties. This extension allows the unearthing of hidden relationships between firing patterns and molecular, biophysical, and morphological data in hippocampal neurons, which are otherwise difficult to find amongst the large body of literature. Several interesting examples of such findings are presented in Box 1. For instance, adapting spiking (ASP.) tends to co-occur with expression of cholecystokinin ($p=0.0113$ with Barnard's exact test from all $n = 26$ pieces of evidence); moreover among 284 analyzed recordings there are no neurons with extremely high input resistance that show persistent stuttering (PSTUT) ($p=0.0478$).

[Box 1 is near here]

520 *Analysis of numerical electrophysiological data.* The extracted quantitative data
521 allow one to study the relationship between firing pattern parameters and membrane
522 biophysics or spike characteristics, such as the correlations between minimum inter-spike
523 intervals (ISI_{min}) and action potential width (AP_{width}). We analyzed these two variables in
524 the 81 neuron types and subtypes for which both measurements are available (Fig. 8).
525 The scatter plot of AP_{width} against ISI_{min} reveals several distinct groupings (Fig. 8A), and
526 the corresponding histograms (Figs. 8B,C) demonstrate poly-modal distributions. The
527 horizontal dashed line (ISI_{min}=34 ms) separates 9 neurons with slow spikes (all excitatory
528 except one) from 72 neurons (61% of which are inhibitory) with fast and moderate spikes.
529 The latter group shows a general trend of ISI_{min} rise with increasing AP_{width} (black dashed
530 line in panel A). This trend was adequately fit with a linear function Y = 13.79X - 0.05 (R
531 = 0.72; p=0.03). Neuron types with slow spikes demonstrate the opposite trend, which
532 was fit with a decreasing linear function Y = - 26.72X + 76.42 (R = -0.91, $p=10^{-6}$).
533 Furthermore, the neuron types can be separated by spike width. The vertical dashed lines
534 *w1* (AP_{width}=0.73 ms) and *w2* (AP_{width}=1.12 ms) separate neuron types with narrow,
535 medium and wide action potentials. The group of neuron types with narrow spikes (n=22)
536 includes only inhibitory neurons, which have AP_{width} in the range from 0.20 to 0.73 ms
537 (0.54 ± 0.12 ms). In contrast, the group of neuron types with wide spikes (n=28) contains
538 only excitatory neurons with AP_{width} in the range from 1.13 to 2.10 ms (1.49 ± 0.23 ms).
539 The group of neuron types with medium spikes (n = 31), with AP_{width} range from 0.74 to
540 1.12 ms (0.89 ± 0.12 ms), includes a mix of inhibitory (74%) and excitatory (26%) neurons.

541 [Figure 8 is near here]

Among the 22 neuron types/subtypes from the group with AP_{width}<0.72 ms, 13 demonstrated so-called fast spiking behavior, which is distinguished by narrow spikes, high firing rate, and the absence or weak expression of spike frequency adaptation (Jonas et al., 2004). Besides these common characteristics, however, their firing patterns vary broadly even from a qualitative standpoint. Five of these 13 neuron types belong to the PSTUT family, namely CA3 Trilaminar (Gloveli et al., 2005), CA3 Aspiny Lucidum ORAX (Spruston et al., 1997), CA2 Basket (Mercer et al., 2007), CA1 Axo-axonic (Pawelzik et al., 2002), and CA1 Radial Trilaminar (Tricoire et al., 2011). Three types belong to the NASP family: DG Basket (Savanthrapadian et al., 2014), CA1 Horizontal Axo-axonic (Tricoire et al, 2011), and MEC LIII Superficial Multipolar Interneuron (Kumar and Buckmaster 2006). Two types, CA3 Axo-axonic (Dugladze et al., 2012) and CA2 Bistratified (Mercer et al., 2007), belong to the simple adapting spiking family; two types, DG HICAP (Mott et al., 1997) and DG AIPRIM (Lubke et al, 1998; Scharfman 1992), belong to the ASP-NASP family; and lastly CA1 Basket (Lee et al., 2011) belongs to non-persistent stuttering family.

Additionally, firing pattern families are unequally distributed among the groupings revealed by the above analysis. Persistent and non-persistent stuttering families and non-persistent bursting phenotypes are composed entirely of neuron types with narrow and medium fast/moderate spikes. Conversely, the rapidly adapting – non-adapting spiking phenotype is represented solely by neurons with spikes of intermediate width.

Discussion

Neurons differ from each other by morphological and molecular features including the diversity and distribution of ion membrane channels in somata and dendrites. These intrinsic properties determine important physiological functions such as excitability, efficacy of synaptic inputs (Häusser et al., 2000; London et al., 2002; Komendantov and Ascoli, 2009), shapes of individual action potentials and their frequency (Bean, 2007), and temporal patterns (Mainen and Sejnowski, 1996; Krichmar et al., 2006).

In the neuroscience literature, the firing patterns of neuronal activity are commonly used to characterize or identify groups of neurons. Examples include descriptions of "strongly adapting, normally adapting, and nonadapting cells" (Mott et al., 1997); "fast-spiking and non-fast-spiking" interneurons (Bjorefeldt et al., 2016); "late spiking" cells (Tamas et al., 2003); "stuttering interneurons" (Song et al., 2013); "bursting" and "non-bursting" neurons (Hablitz and Johnston, 1981; Maskawa et al., 1982); "regular spiking, bursting, and fast spiking" (McCormick et al., 1985), and many more. However, it has until now remained challenging to integrate these characterizations across different laboratories and studies besides largely qualitative summaries.

In this study, we show that a quantitative, data-driven methodology based on the analysis of transients and steady states of evoked spiking activity can meaningfully classify the firing patterns of hippocampal neuronal types. This work is a further development of the effort initiated by the Petilla Interneuron Nomenclature Group (2008), which was applied to firing patterns in cortical neurons (Druckmann et al., 2013; Markram et al., 2015). At the same time, this work demonstrates the feasibility of systematic, comprehensive meta-analysis of electrophysiological data from the published literature.

586 This is especially important as a necessary approach to help link and interpret the growing
587 information from centralized, large-scale, "industrial" neuroscience projects (Kandel et al.,
588 2013; Migliore et al., 2018; Teeter et al., 2018), with the distributed accumulation of data
589 in traditional research laboratories (Ferguson et al., 2014).

590 From the electrophysiological recordings of 90 neuron types in the rodent
591 hippocampus, we identified 23 firing patterns, 15 of which were completed, that is,
592 included both transient(s) and putative steady state components (see Figs. 4 and 5).
593 Taking into consideration the firing pattern information enables a possible refinement of
594 neuron type delineation by identifying 52 putative electrophysiological subtypes among
595 22 neuron types. Subsequent two-step cluster analysis allows for the clear distinguishing
596 of 9 unique families of 44 firing pattern phenotypes among 120 neuron types and putative
597 subtypes. Notwithstanding the focus of the present research on the hippocampal
598 formation, the firing pattern classification framework introduced with this study can be
599 readily applied to spiking activity of neurons from other brain regions.

600 The two firing pattern families characterized by bursting phenotypes (transient and
601 persistent) are comprised of excitatory neurons, while the persistent stuttering family only
602 included inhibitory neurons. However, the majority of phenotype families are mixed
603 between putatively glutamatergic and GABAergic types (Fig. 6B). Thus, the identification
604 of a firing pattern phenotype by itself is a useful but in most cases insufficient attribute for
605 a reliable categorization of excitatory and inhibitory neurons.

606 The frequency of discharges is an important characteristic of neuronal
607 communication. Many neuron types, especially interneurons, show fast spiking behavior:

608 they are capable of firing at high frequencies (200 Hz or more) with little decrease in
609 frequency during prolonged stimulation (Jonas et al., 2004; Bean 2007). Spike frequency
610 correlates with electrophysiological characteristics, such as action potential duration or
611 fast AHP amplitude (Druckmann et al., 2013). Fast spiking neurons typically have narrow
612 action potentials and high-amplitude fast AHP (Bean 2007). Our correlation analysis of
613 Hippocampome.org data reveals that transient stuttering (TSTUT.) is not typical for cells
614 with extremely high-amplitude fast AHPs and delayed firing (D.) is not characteristic for
615 neuron types with wide action potentials (Box 1). Interestingly, plotting ISI_{min} against
616 AP_{width} for all neuron types with relatively faster firing (maximum frequencies higher than
617 ~30 Hz) and for all neuron types with slower firing (maximum frequencies lower than 29
618 Hz) reveals opposite, statistically significant linear relationships (Fig. 8A).

619 Firing pattern phenotypes of central mammalian neurons are determined by
620 biophysical properties associated with expression and distribution of several types of Ca^{2+}
621 and K^+ channels, which modulate specific ion currents (Llinás 1988; Migliore and
622 Shepherd, 2005; Bean, 2007), as well as with expression of other molecular markers
623 (Caballero et al., 2014; Markram et al., 2004; Petilla Interneuron Nomenclature Group et
624 al., 2008). Despite the relative sparsity of molecular marker information, analysis of the
625 correlations between firing patterns and other neuronal properties revealed novel
626 interesting relationships in hippocampal neuron types (see Box 1 for illustrative
627 examples).

628 Firing patterns play important roles in neural networks including the representation
629 of input features, transmission of information, and synchronization of activity across

separate anatomical regions or distinct cell assemblies. Although single spikes can provide temporally precise neurotransmitter release, this release usually has low probability in central synapses. Neurons can compensate for the unreliability of their synapses by transmitting signals via multiple synaptic endings or repeatedly activating a single synapse (Lisman, 1997). Thus, spikes grouped together in bursting or stuttering activity increase the probability of transmission via unreliable synapses compared to separate spikes with the same average frequency. In the hippocampus, a single burst can produce long-term synaptic potentiation or depression (Lisman, 1997). It has also been hypothesized that, due to the interplay between short-term synaptic depression and facilitation, bursting with certain values of ISIs are more likely to cause a postsynaptic cell to fire than bursts with higher or lower frequencies (Izhikevich et al., 2003). Recent results have also revealed that single bursts in hippocampal neurons may selectively alter specific functional components of the downstream circuit, such as feedforward inhibitory interneurons (Neubrandt et al., 2018).

Experimental studies provide strong evidence that different brain circuits employ distinct schemes to encode and propagate information (Xu et al, 2012): while information relay by isolated spikes is insignificant for the acquisition of recent contextual memories in the hippocampus, it is essential for memory function in the medial prefrontal cortex. However, even within the hippocampus, different neuronal circuits may employ distinct coding schemes by relying on isolated spikes or bursts of spikes for execution of critical functions (Xu et al, 2012). Indeed, distinct sub-regions of the hippocampal formation show differential distributions of spiking, bursting, and stuttering firing pattern phenotypes (Fig. 6).

In this study, the phenotyping of most types of neurons was relied on the digitization and quantitative analysis of single (or limited numbers of) experimental recordings of electrical activity extracted from many relevant publications. Until neuroscience switches to the systematic deposition of all firing traces recorded and analyzed for a given publication to public repositories, such representative illustrations, however limited, constitute a fairly accurate reflection of the communal knowledge about neuronal physiology in particular neural system. Thus, our approach is based on the statistical quantification of integrated data presented in the literature.

The findings presented in this report resulted from the analysis of firing patterns in response to depolarizing current. To this date, this is by far the most common experimental protocol for characterizing the neuronal input-output function. Nevertheless, different types of neurons also exhibit distinct responses to hyperpolarization, as well as to its termination. For example, several neuron types described in Hippocampome.org demonstrate rebound spiking: CA1 Trilaminar (Tricoire et al., 2011, Sik et al., 1995), CA1 Back-Projection (Sik et al., 1994), CA1 O-LM (Sik et al., 1995), CA1 SO-SO (Pawelzik et al., 2002), MEC LIII Multipolar Interneuron (Kumar and Buckmaster 2006), MEC LII Stellate (Canto and Witter 2012b), MEC LII Oblique Pyramidal (Canto and Witter 2012b). Such neuronal behaviors, owing to the hyperpolarization-activated cation current (h-current), may play an important role in hippocampal rhythmogenesis (raHasselmo 2014) and could be locally modulated by activity-dependent changes in intrinsic excitability (Ascoli et al., 2010). It will therefore be interesting to extend the current firing pattern phenotyping by considering these additional neuronal properties in future work.

675 The information on firing patterns of neuron types further expands the rich
676 knowledge base of neuronal properties Hippocampome.org, which already contained
677 information on morphology, molecular marker expression, connectivity, and other
678 electrophysiological characteristics (Wheeler et al., 2015). Computation of the potential
679 connectivity map of all known 122 neuron types by supplementing available synaptic data
680 with spatial distributions of axons and dendrites enabled the reconstruction of a circuitry
681 containing more than 3200 putative connections (Rees et al., 2016).

682 Further development also includes simulation of firing activity of different neuron
683 types based on dynamical systems modeling (Venkadesh et al., 2018). This ongoing
684 accumulation of data and knowledge makes Hippocampome.org a powerful tool for
685 building real-scale models of the entire hippocampal formation, thus substantially
686 expanding the potential scope of recent advances in this regard (Bezaire et al., 2016).
687 More generally, such knowledge bases are playing an increasingly important role in
688 neuroscience research by fostering computational analyses and data-driven simulations.

689

690 **References**

691 Adrian ED, Zotterman Y (1926) The impulses produced by sensory nerve endings: Part
692 3. Impulses set up by touch and pressure. J Physiol 61:465-483.

693

694 Ali AB, Thomson AM (1998) Facilitating pyramid to horizontal oriens-alveus interneurone
695 inputs: dual intracellular recordings in slices of rat hippocampus. J Physiol 507:185-199.

Armstrong C, Szabadics J, Tamás G, Soltesz I (2011) Neurogliaform cells in the molecular layer of the dentate gyrus as feed-forward γ-aminobutyric acidergic modulators of entorhinal-hippocampal interplay. J Comp Neurol 519:1476-1491.

Ascoli GA, Brown KM, Calixto E, Card JP, Galván EJ, Perez-Rosello T, Barrionuevo G (2009) Quantitative morphometry of electrophysiologically identified CA3b interneurons reveals robust local geometry and distinct cell classes. J Comp Neurol 515:677-695.

Ascoli GA, Gasparini S, Medinilla V, Migliore M (2010) Local control of postinhibitory rebound spiking in CA1 pyramidal neuron dendrites. J Neurosci 30:6434-6442.

Barnard GA (1947) Significance tests for 2×2 tables. Biometrika 34:123–138.

Bean BP (2007) The action potential in mammalian central neurons. Nat Rev Neurosci 8:451-465.

Bezaire MJ, Raikov I, Burk K, Vyas D, Soltesz I (2016) Interneuronal mechanisms of

714 hippocampal theta oscillations in a full-scale model of the rodent CA1 circuit. Elife 5:
715 e18566. doi: 10.7554/eLife.18566.

716

717 Bilkey DK, Schwartzkroin PA (1990) Variation in electrophysiology and morphology of
718 hippocampal CA3 pyramidal cells. Brain Res 514:77-83.

719

720 Bjorefeldt A, Wasling P, Zetterberg H, Hanse E (2016) Neuromodulation of fast-spiking
721 and non-fast-spiking hippocampal CA1 interneurons by human cerebrospinal fluid. J
722 Physiol 594:937-952.

723

724 Buchanan TW (2007) Retrieval of emotional memories. Psychol Bull 133: 761-779.

725

726 Buhl EH, Han ZS, Lörinczi Z, Stezhka VV, Karnup SV, Somogyi P (1994) Physiological
727 properties of anatomically identified axo-axonic cells in the rat hippocampus. J
728 Neurophysiol 71:1289-1307.

729

730 Bullis JB, Jones TD, Poolos NP (2007) Reversed somatodendritic I(h) gradient in a class
731 of rat hippocampal neurons with pyramidal morphology. J Physiol 579:431-443.

732

733 Caballero A, Flores-Barrera E, Cass DK, Tseng KY (2014) Differential regulation of
734 parvalbumin and calretinin interneurons in the prefrontal cortex during adolescence. Brain
735 Struct Funct 219:395-406.

736

737 Canto CB, Witter MP (2012a) Cellular properties of principal neurons in the rat entorhinal
738 cortex. I. The lateral entorhinal cortex. Hippocampus 22:1256-1276.

739

740 Canto CB, Witter MP (2012b) Cellular properties of principal neurons in the rat entorhinal
741 cortex. II. The medial entorhinal cortex. Hippocampus 22:1277-1299.

742

743 Chevaleyre V, Siegelbaum SA (2010) Strong CA2 pyramidal neuron synapses define a
744 powerful disynaptic cortico-hippocampal loop. Neuron 66:560-572.

745

746 Connors BW, Gutnick MJ (1990) Intrinsic firing patterns of diverse neocortical neurons.
747 Trends Neurosci 13:99-104.

748

749 Druckmann S, Hill S, Schürmann F, Markram H, Segev I (2013) A hierarchical structure
750 of cortical interneuron electrical diversity revealed by automated statistical analysis.
751 Cereb Cortex 23:2994-3006.

Dugladze T, Schmitz D, Whittington MA, Vida I, Gloveli T (2012) Segregation of axonal and somatic activity during fast network oscillations. Science 336:1458-1461.

Eichenbaum H (2000) A cortical-hippocampal system for declarative memory. Nat Rev Neurosci 1:41-50.

Eichenbaum H (2017) The role of the hippocampus in navigation is memory. J Neurophysiol. 117:1785-1796.

Eichenbaum H, Otto T, Cohen NJ (1992) The hippocampus - what does it do? Behav Neural Biol 57:2-36.

Ferguson AR, Nielson JL, Cragin MH, Bandrowski AE, Martone ME (2014) Big data from small data: data-sharing in the 'long tail' of neuroscience. Nat Neurosci 17:1442-1447.

Ferster D, Spruston N (1995) Cracking the neuronal code. Science 270:756-757.

770 Fuentealba P, Klausberger T, Karayannis T, Suen WY, Huck J, Tomioka R, Rockland K,
771 Capogna M, Studer M, Morales M, Somogyi P (2010) Expression of COUP-TFII nuclear
772 receptor in restricted GABAergic neuronal populations in the adult rat hippocampus. J
773 Neurosci 30:1595-1609.

774

775 Gloveli T, Dugladze T, Saha S, Monyer H, Heinemann U, Traub RD, Whittington MA, Buhl
776 EH (2005) Differential involvement of oriens/pyramidale interneurones in hippocampal
777 network oscillations *in vitro*. J Physiol 562:131-147.

778

779 Golomb D, Donner K, Shacham L, Shlosberg D, Amitai Y, Hansel D (2007) Mechanisms
780 of firing patterns in fast-spiking cortical interneurons. PLoS Comput Biol 3(8):e156. doi:
781 10.1371/journal.pcbi.0030156.

782

783 Golomb D, Yue C, Yaari Y (2006) Contribution of persistent Na^+ current and M-type K^+
784 current to somatic bursting in CA1 pyramidal cells: combined experimental and modeling
785 study. J Neurophysiol 96:1912-1926.

786

787 Gulyás AI, Szabó GG, Ulbert I, Holderith N, Monyer H, Erdélyi F, Szabó G, Freund TF,
788 Hájos N (2010) Parvalbumin-containing fast-spiking basket cells generate the field

789 potential oscillations induced by cholinergic receptor activation in the hippocampus. J
790 Neurosci 30:15134-15145.

791

792 Hablitz JJ, Johnston D (1981) Endogenous nature of spontaneous bursting in
793 hippocampal pyramidal neurons. Cell Mol Neurobiol 1:325-334.

794

795 Hafting T, Fyhn M, Molden S, Moser MB, Moser EI (2005) Microstructure of a spatial map
796 in the entorhinal cortex. Nature 436:801-806.

797

798 Hamam BN, Kennedy TE, Alonso A, Amaral DG (2000) Morphological and
799 electrophysiological characteristics of layer V neurons of the rat medial entorhinal cortex.
800 J Comp Neurol 418:457-472.

801

802 Hamam BN, Amaral DG, Alonso AA (2002) Morphological and electrophysiological
803 characteristics of layer V neurons of the rat lateral entorhinal cortex. J Comp Neurol
804 451:45-61.

805

806 Hamilton DJ, Wheeler DW, White CM, Rees CL, Komendantov AO, Bergamino M, Ascoli
807 GA (2017) Name-calling in the hippocampus (and beyond): coming to terms with neuron
808 types and properties. Brain Inform 4:1-12.

Han ZS, Buhl EH, Lörinczi Z, Somogyi P (1993) A high degree of spatial selectivity in the axonal and dendritic domains of physiologically identified local-circuit neurons in the dentate gyrus of the rat hippocampus. Eur J Neurosci 5:395-410.

Hasselmo ME (2014) Neuronal rebound spiking, resonance frequency and theta cycle skipping may contribute to grid cell firing in medial entorhinal cortex. Phil Trans R Soc B 369: 20120523. doi:10.1098/rstb.2012.0523

Häusser M, Spruston N, Stuart GJ (2000) Diversity and dynamics of dendritic signaling. Science 290:739-744.

Hayward LF, Felder RB (1999) Electrophysiological properties of rat lateral parabrachial neurons in vitro. Am J Physiol 276:R696-R706.

Hemond P, Epstein D, Boley A, Migliore M, Ascoli GA, Jaffe DB (2008) Distinct classes of pyramidal cells exhibit mutually exclusive firing patterns in hippocampal area CA3b. Hippocampus 18:411-424.

828 Izhikevich EM, Desai NS, Walcott EC, Hoppensteadt FC (2003) Bursts as a unit of neural
829 information: selective communication via resonance. Trends Neurosci 26(3):161-167.

830

831 Jonas P, Bischofberger J, Fricker D, Miles R (2004) Interneuron diversity series: fast in,
832 fast out-temporal and spatial signal processing in hippocampal interneurons. Trends
833 Neurosci 27:30-40.

834

835 Kandel ER, Markram H, Matthews PM, Yuste R, Koch C (2013) Neuroscience thinks big
836 (and collaboratively). Nat Rev Neurosci 14:659-664.

837

838 Kirson ED, Yaari Y (2000) Unique properties of NMDA receptors enhance synaptic
839 excitation of radiatum giant cells in rat hippocampus. J Neurosci 20:4844-4854.

840

841 Komendantov AO, Ascoli GA (2009) Dendritic excitability and neuronal morphology as
842 determinants of synaptic efficacy. J Neurophysiol 2009 101:1847-166.

843

844 Krichmar JL, Velasquez D, Ascoli GA (2006) Effects of beta-catenin on dendritic
845 morphology and simulated firing patterns in cultured hippocampal neurons. Biol Bull
846 211:31-43.

847

Kumar SS, Buckmaster PS (2006) Hyperexcitability, interneurons, and loss of GABAergic synapses in entorhinal cortex in a model of temporal lobe epilepsy. J Neurosci 26:4613-4623.

Lee SY, Földy C, Szabadics J, Soltesz I (2011) Cell-type-specific CCK2 receptor signaling underlies the cholecystokinin-mediated selective excitation of hippocampal parvalbumin-positive fast-spiking basket cells. J Neurosci 31:10993-11002.

Leroy F, Lamotte d'Incamps B, Imhoff-Manuel RD, Zytnicki D (2014) Early intrinsic hyperexcitability does not contribute to motoneuron degeneration in amyotrophic lateral sclerosis. eLife 3:e04046 doi: 10.7554/eLife.04046.

Lien CC, Jonas P (2003) Kv3 potassium conductance is necessary and kinetically optimized for high-frequency action potential generation in hippocampal interneurons. J Neurosci 23:2058-2068.

Lisman JE (1997) Bursts as a unit of neural information: making unreliable synapses reliable. Trends Neurosci 20:38-43.

Llinás RR. (1988) The intrinsic electrophysiological properties of mammalian neurons: insights into central nervous system function. Science 242:1654-1664.

London M, Schreibman A, Häusser M, Larkum ME, Segev I (2002) The information efficacy of a synapse. Nat Neurosci 5:332-340.

Lübke J, Frotscher M, Spruston N (1998) Specialized electrophysiological properties of anatomically identified neurons in the hilar region of the rat fascia dentata. J Neurophysiol 79:1518-1534.

Lydersen S, MW Fagerland MF, Laake P (2009) Recommended tests for association in 2 × 2 tables. Statistics in Medicine 28:1159-1175.

Mainen ZF, Sejnowski TJ (1996) Influence of dendritic structure on firing pattern in model neocortical neurons. Nature 382:363-366.

Masukawa LM, Benardo LS, Prince DA (1982) Variations in electrophysiological properties of hippocampal neurons in different subfields. Brain Res 242: 341–344.

Markram H, Toledo-Rodriguez M, Wang Y, Gupta A, Silberberg G, Wu C (2004) Interneurons of the neocortical inhibitory system. Nat Rev Neurosci 5:793-807.

Markram H, Muller E, Ramaswamy S, Reimann MW, Abdellah M, Sanchez CA, Ailamaki A, Alonso-Nanclares L, Antille N, Arsever S, Kahou GA, Berger TK, Bilgili A, Buncic N, Chalimourda A, Chindemi G, Courcol JD, Delalondre F, Delattre V, Druckmann S, Dumusc R, Dynes J, Eilemann S, Gal E, Gevaert ME, Ghobril JP, Gidon A, Graham JW, Gupta A, Haenel V, Hay E, Heinis T, Hernando JB, Hines M, Kanari L, Keller D, Kenyon J, Khazen G, Kim Y, King JG, Kisvarday Z, Kumbhar P, Lasserre S, Le Bé JV, Magalhães BR, Merchán-Pérez A, Meystre J, Morrice BR, Muller J, Muñoz-Céspedes A, Muralidhar S, Muthurasa K, Nachbaur D, Newton TH, Nolte M, Ovcharenko A, Palacios J, Pastor L, Perin R, Ranjan R, Riachi I, Rodríguez JR, Riquelme JL, Rössert C, Sfyrakis K, Shi Y, Shillcock JC, Silberberg G, Silva R, Tauheed F, Telefont M, Toledo-Rodriguez M, Tränkler T, Van Geit W, Díaz JV, Walker R, Wang Y, Zaninetta SM, DeFelipe J, Hill SL, Segev I, Schürmann F (2015) Reconstruction and Simulation of Neocortical Microcircuitry. Cell 163:456-492.

McCormick DA, Connors BW, Lighthall JW, Prince DA (1985) Comparative electrophysiology of pyramidal and sparsely spiny stellate neurons of the neocortex. J Neurophysiol 54:782-806.

McNaughton BL, Barnes CA, O'Keefe J (1983) The contributions of position, direction, and velocity to single unit activity in the hippocampus of freely-moving rats. Exp Brain Res 52:41-49.

Mercer A, Trigg HL, Thomson AM (2007) Characterization of neurons in the CA2 subfield of the adult rat hippocampus. J Neurosci 27:7329-7338.

Mercer A, Botcher NA, Eastlake K, Thomson AM (2012) SP-SR interneurones: a novel class of neurones of the CA2 region of the hippocampus. Hippocampus 22:1758-1769.

Migliore M, Shepherd GM. (2005) Opinion: an integrated approach to classifying neuronal phenotypes. Nat Rev Neurosci 6:810-818.

Migliore R, Lupascu CA, Bologna LL, Romani A, Courcol JD, Antonel S, Van Geit WAH, Thomson AM, Mercer A, Lange S, Falck J, Rössert CA, Shi Y, Hagens O, Pezzoli M, Freund TF, Kali S, Muller EB, Schürmann F, Markram H, Migliore M (2018) The physiological variability of channel density in hippocampal CA1 pyramidal cells and interneurons explored using a unified data-driven modeling workflow. PLoS Comput Biol doi: 10.1371/journal.pcbi.1006423.

927 Mott DD, Turner DA, Okazaki MM, Lewis DV (1997) Interneurons of the dentate-hilus
928 border of the rat dentate gyrus: morphological and electrophysiological heterogeneity. J
929 Neurosci 17:3990-4005.

930

931 Neubrandt M, Oláh VJ, Brunner J, Marosi EL, Soltesz I, Szabadics J (2018) Single bursts
932 of individual granule cells functionally rearrange feedforward inhibition. J Neurosci
933 38:1711-1724.

934

935 O'Keefe J, Dostrovsky J (1971) The hippocampus as a spatial map. Preliminary evidence
936 from unit activity in the freely-moving rat. Brain Res 34:171-175.

937

938 Pawelzik H, Hughes DI, Thomson AM (2002) Physiological and morphological diversity
939 of immunocytochemically defined parvalbumin- and cholecystokinin-positive
940 interneurones in CA1 of the adult rat hippocampus. J Comp Neurol 443:346-367.

941

942 Petilla Interneuron Nomenclature Group., Ascoli GA, Alonso-Nanclares L, Anderson SA,
943 Barrionuevo G, Benavides-Piccione R, Burkhalter A, Buzsáki G, Cauli B, Defelipe J,
944 Fairén A, Feldmeyer D, Fishell G, Fregnac Y, Freund TF, Gardner D, Gardner EP,
945 Goldberg JH, Helmstaedter M, Hestrin S, Karube F, Kisvárday ZF, Lambolez B, Lewis
946 DA, Marin O, Markram H, Muñoz A, Packer A, Petersen CC, Rockland KS, Rossier J,

947 Rudy B, Somogyi P, Staiger JF, Tamas G, Thomson AM, Toledo-Rodriguez M, Wang Y,
948 West DC, Yuste R (2008) Petilla terminology: nomenclature of features of GABAergic
949 interneurons of the cerebral cortex. Nat Rev Neurosci 9:557-568.

950

951 Price CJ, Cauli B, Kovacs ER, Kulik A, Lambolez B, Shigemoto R, Capogna M (2005)
952 Neurogliaform neurons form a novel inhibitory network in the hippocampal CA1
953 area. J Neurosci 25:6775-6786.

954

955 Rees CL, Wheeler DW, Hamilton DJ, White CM, Komendantov AO, Ascoli GA (2016)
956 Graph theoretic and motif analyses of the hippocampal neuron type potential
957 connectome. eNeuro 3. pii: ENEURO.0205-16.2016.

958

959 Rinzel J, Ermentrout GB (1998) Analysis of neural excitability and oscillations. In: Koch
960 C, Segev I, editors. Methods in neuronal modeling: From ions to networks. 2nd edition.
961 Cambridge (Massachusetts): MIT Press. pp. 251–291.

962

963 Rudy B, McBain CJ (2001) Kv3 channels: voltage-gated K^+ channels designed for
964 high-frequency repetitive firing. Trends Neurosci 24:517-526.

965

966 Rudy JW, Sutherland RJ (1989) Configural association theory: The role of the
967 hippocampal formation in learning, memory, and amnesia. Psychobiology 17: 129–144.
968
969 Rudy JW, Sutherland RJ (1995) Configural association theory and the hippocampal
970 formation: an appraisal and reconfiguration. Hippocampus 5:375-389.
971
972 Savanthrapadian S, Meyer T, Elgueta C, Booker SA, Vida I, Bartos M (2014) Synaptic
973 properties of SOM- and CCK-expressing cells in dentate gyrus interneuron networks. J
974 Neurosci 34:8197-8209.
975
976 Sciamanna G, Wilson CJ (2011) The ionic mechanism of gamma resonance in rat striatal
977 fast-spiking neurons. J Neurophysiol 106:2936-2949.
978
979 Sik A, Ylinen A, Penttonen M, Buzsáki G (1994) Inhibitory CA1-CA3-hilar region feedback
980 in the hippocampus. Science 265:1722-1724.
981
982 Sik A, Penttonen M, Ylinen A, Buzsáki G (1995) Hippocampal CA1 interneurons: an in
983 vivo intracellular labeling study. J Neurosci 15:6651-6665.
984

985 Smith M, Perrier JF (2006) Intrinsic properties shape the firing pattern of ventral horn
986 interneurons from the spinal cord of the adult turtle. J Neurophysiol 96:2670-2677.

987

988 Song C, Xu XB, He Y, Liu ZP, Wang M, Zhang X, Li BM, Pan BX (2013) Stuttering
989 interneurons generate fast and robust inhibition onto projection neurons with low capacity
990 of short term modulation in mouse lateral amygdala. PLoS One 8:e60154.

991

992 Spruston N, Lübke J, Frotscher M (1997) Interneurons in the stratum lucidum of the rat
993 hippocampus: an anatomical and electrophysiological characterization. J Comp Neurol
994 385:427-440.

995

996 Staff NP, Jung HY, Thiagarajan T, Yao M, Spruston N (2000) Resting and active
997 properties of pyramidal neurons in subiculum and CA1 of rat hippocampus. J
998 Neurophysiol 84:2398-2408.

999

1000 Szabadics J and Soltesz I (2009) Functional specificity of mossy fiber innervation of
1001 GABAergic cells in the hippocampus. J Neurosci 29:4239-4251.

1002

1003 Tamas G, Lorincz A, Simon A, Szabadics J (2003) Identified sources and targets of slow
1004 inhibition in the neocortex. Science 299:1902-1905.

Tebaykin D, Tripathy SJ, Binnion N, Li B, Gerkin RC, Pavlidis P (2018) Modeling sources of interlaboratory variability in electrophysiological properties of mammalian neurons. J Neurophysiol 119:1329-1339.

Teeter C, Iyer R, Menon V, Gouwens N, Feng D, Berg J, Szafer A, Cain N, Zeng H, Hawrylycz M, Koch C, Mihalas S (2018). Generalized leaky integrate-and-fire models classify multiple neuron types. Nat Commun 9:709.

Tripathy SJ, Burton SD, Geramita M, Gerkin RC, Urban NN (2015) Brain-wide analysis of electrophysiological diversity yields novel categorization of mammalian neuron types. J Neurophysiol 113:3474-3489.

Tricoire L, Pelkey KA, Erkkila BE, Jeffries BW, Yuan X, McBain CJ (2001) A blueprint for the spatiotemporal origins of mouse hippocampal interneuron diversity. J Neurosci 31:10948-10970.

Venkadesh S, Komendantov AO, Listopad S, Scott EO, De Jong K, Krichmar JL, Ascoli GA (2018) Evolving simple models of diverse intrinsic dynamics in hippocampal neuron types. Front Neuroinform 12:8. doi:10.3389/fninf.2018.00008.

Vida I, Halasy K, Szinyei C, Somogyi P, Buhl EH (1998) Unitary IPSPs evoked by interneurons at the stratum radiatum-stratum lacunosum-moleculare border in the CA1 area of the rat hippocampus in vitro. J Physiol 506:755-773.

Williams PA, Larimer P, Gao Y, Strowbridge BW (2007) Semilunar granule cells: glutamatergic neurons in the rat dentate gyrus with axon collaterals in the inner molecular layer. J Neurosci 27:13756 –1376.

Wheeler DW, White CM, Rees CL, Komendantov AO, Hamilton DJ, Ascoli GA (2015) Hippocampome.org: a knowledge base of neuron types in the rodent hippocampus. eLife 4:e09960. doi: 10.7554/eLife.09960.

Xu J, Clancy CE (2008) Ionic mechanisms of endogenous bursting in CA3 hippocampal pyramidal neurons: a model study. PLoS One 3:e2056. doi:10.1371/journal.pone.0002056.

Xu W, Morishita W, Buckmaster PS, Pang ZP, Malenka RC, Südhof TC (2012) Distinct neuronal coding schemes in memory revealed by selective erasure of fast synchronous synaptic transmission. Neuron 73:990-1001.

Zemankovics R, Káli S, Paulsen O, Freund TF, Hájos N (2010) Differences in subthreshold resonance of hippocampal pyramidal cells and interneurons: the role of h-current and passive membrane characteristics. J Physiol 588:2109-2132.

Zhao ML, Wu CF (1997) Alterations in frequency coding and activity dependence of excitability in cultured neurons of *Drosophila* memory mutants. J Neurosci 17:2187-2199.

Legends

Figure 1. Firing pattern elements observable in hippocampal neurons *in vitro*. ISI - inter-spike interval, PFS – post firing silence, sDW – slow depolarization wave, sAHP – slow after-hyperpolarization. Original data extracted from Lübke et al. (1998) (D), Vida et al. (1998) (ASP), Pawelzik et al. (2002) (RASP), Hamam et al. (2002) (TSTUT), Chevaleyre and Seigelbaum (2010) (TSWB), Mercer et al. (2012) (SLN), Mott et al. (1997) (NASP), Fuentealba et al. (2010) (PSTUT), and Golomb et al. (2006) (PSWB, spontaneous bursting in Ca^{2+}-free ACSF).

Figure 2. Examples of fitting of spiking activity with linear regression and piecewise linear regression models. **A.** Responses to current injection of a DG aspiny interneuron

1065 with axonal projection to the inner molecular layer (AIPRIM in Hippocampome.org)
1066 (Original data extracted from Lübke et al., 1998). **B.** Fitting of digitized experimental
1067 data with different models.

1068 1 parameter fit is a constant function Y=2.78;

1069 2 parameter fit is a linear function Y=0.017X+1.67;

1070 3 parameter fit is a piecewise linear function $Y = \begin{cases} 0.031X + 1.27 & if\ X < 74.9 \\ 3.58 & if\ X \geq 74.9 \end{cases}$;

1071 4 parameter fit is a piecewise linear function $Y = \begin{cases} 0.033X + 1.23 & if\ X < 61.3 \\ 0.006X + 2.87 & if\ X \geq 61.3 \end{cases}$.

1072 Based on p-values, the firing pattern was identified as adapting-non-adapting spiking
1073 (ASP.NASP): $p_{2,1} < 0.05$ ($p_{2,1} = 1.26 \cdot 10^{-10}$), $p_{3,2} < 0.025$ ($p_{3,2} = 2.7 \cdot 10^{-3}$), $p_{4,3} > 0.016$
1074 ($p_{4,3} = 5.5 \cdot 10^{-2}$). $p_{2,1}$, $p_{3,2}$, $p_{4,3}$ – p-values of differences between 2 parameter fit and 1
1075 parameter fit, 3 parameter fit and 2 parameter fit, 4 parameter fit and 3 parameter fit,
1076 respectively.

1077

1078 **Figure 3.** Flow chart of general procedure for firing pattern identification. See text for
1079 abbreviations. Source code and executable of Java implementation available at
1080 github.com/Hippocampome-Org/NeuroSpikePatterns.

1081

Figure 4. Identified firing patterns and firing pattern phenotypes complexity of neuron types (**A**) and subtypes (**B**). Online matrix: hippocampome.org/firing_patterns. Green and red cell type/subtype names denote excitatory (e) and inhibitory (i) neurons, respectively. FPP is firing pattern phenotype. The numbers in the brackets correspond to the order in which the cell types were presented in the Hippocampome (ver. 1.3). The orange asterisk denotes different experimental conditions. **C**. Complexity of firing pattern phenotypes; percentages and ratios indicate occurrences of phenotypes of different complexity among 120 cell types/subtypes.

Figure 5. Occurrence of firing patterns, firing pattern elements and firing pattern phenotypes among the hippocampal formation neuron types. **A**. Distribution of 23 firing patterns; total numbers are shown above the bars. **B**. Distribution of 9 firing pattern elements; total numbers are in parentheses below and percentages of occurrence among 90 cell types are above the bars. **C**. Relationships between firing pattern elements in the firing patterns of hippocampal neuron types. Numbers of cell types with distinctive firing patterns are indicated.

Figure 6. Ten firing pattern phenotype families from 120 neuron types/subtypes. **A**. Hierarchical tree resulting from two-step clustering of weighted firing pattern elements with representative examples of cell types/subtypes which belong to corresponding firing pattern phenotype family. Simple adapting firing pattern phenotype is not unique (see *Results*). **B**. Percentage of occurrence of firing pattern elements in families of firing

pattern phenotypes. **C**. Relative proportions of firing pattern phenotypes among neuron types/subtypes. Green and red numbers represent excitatory and inhibitory cell types/subtypes as enumerated in Fig. 4. **D**. Distribution of firing pattern phenotypes in sub-regions of the hippocampal formation. FPP% is percentage of expression of firing pattern phenotypes.

Figure 7. Hippocampome.org enables searching neuron types by neurotransmitter; axon, dendrite, and soma locations; molecular expression; electrophysiological parameters; input/output connectivity; firing patterns, and firing pattern parameters. **A**. Sample query for calbindin-negative neuron types with axons in CA1 stratum pyramidale, AP_{width} <0.8 ms, PSTUT firing, and ratio of maximum ISI to the next ISI greater than 4.8. Numbers in parentheses indicate the number of neuron types with the selected property or specific combination of properties. **B**. Search results are linked to the neuron page(s). **C**. The neuron page is linked to the firing pattern evidence page. Original data extracted from Pawelzik et al., 2002. **D-H.** All firing patterns parameters (**D**), experimental details including information about animals (**E**), preparations (**F**), recording method and intra-pipette solution (**G**), as well as ACSF composition (**H**) can be displayed. **I.** Downloadable comma-separated-value file of inter-spike intervals.

Figure 8. Relationships between the width of action potentials (AP_{width}) and minimum of inter-spike intervals (ISI_{min}) for 84 neuron types and subtypes. **A.** AP_{width} - ISI_{min} scatter diagram with results of linear regression. Green triangles and red circles indicate

1126 excitatory and inhibitory neurons, respectively. Dashed orange lines: horizontal line
1127 separates neurons with slow spikes from neurons with fast and moderate spikes; vertical
1128 lines (*w1* and *w2*) separate neurons with narrow, medium and wide action potentials.
1129 Black lines: solid line shows linear fitting for slow spike neurons with a function Y = -
1130 26.72X + 76.42 (R^2=0.83); dashed lie shows general linear fitting for fast and moderate
1131 spike neurons with a function Y = 13.79X - 0.05 (R^2=0.52). **B**. AP_{width} histogram. **C**. ISI
1132 histogram.

1133

1134 **Table 1. Abbreviations:** Pct. – percentage of firing pattern recordings for which this
1135 solution was used.

1136

1137 **Table 2. Abbreviations:** KAc – potassium acetate (KCH_3COO); KGlu – potassium
1138 gluconate; $KMeSO_4$ – potassium methylsulphate (CH_3KSO_4); PCr – phosphocreatine;
1139 Pct. – percentage of firing pattern recordings for which this solution was used; 10 mM
1140 HEPES (4-(2-hydroxyethyl)-1-piperazineethanesulfonic acid) was used in all patch
1141 pipette solutions. Asterisks indicate examples of micropipette solutions.

1142

1143 **Table 3. Abbreviations:** a_1 – slope of linear fitting for normalized ISIs *vs* normalized
1144 time; *DF* – delay factor; f_{min} – minimum frequency of stuttering or bursting; F_{pre}, F_{post} ,
1145 F_{PSTUT} , F_{PSWB} – ISI comparison factors, ISI_{max} –maximum inter-spike interval; $p_{2,1}$ – *p*-
1146 value for differences between two- and one-parameter linear fitting; $p_{3,2}$ – *p*-value for

differences between three- and two-parameter linear fitting; *PFS* – post firing silence; *SF* – silence factor; S_{RASP} – slope of linear fitting of rapid transient; *SWA* – slow wave amplitude; SWA_{min} – minimum slow wave amplitude.

Table 4. NASP – HICAP (Mott et al. 1997, Fig. 11A); **PSTUT** - CA1 Neurogliaform (Fuentealba et al. 2010, Fig.5B); **PSWB** - CA3 Pyramidal (Bilkey and Schwartzkroin 1990, Fig. 1a); **ASP.NASP** - CA3 Basket-CCK (Gulyás et al. 2010, Fig. 1b, right); **ASP.SLN** – EC MEC LV Pyramidal (Canto and Witter 2012b, Fig.10C7); **RASP.NASP** – EC LV Deep Pyramidal (Hamam et al. 2000, Fig.3C); **RASP.SLN** – CA1 Radiatum Giant (Bullis et al. 2007, Fig.5A); **TSTUT.NASP** - EC LV Deep Pyramidal (Hamam et al. 2002, Fig.5E); **TSTUT.PSTUT** - CA1 (Price et al. 2005, Fig.3A2); **TSUT.SLN** – CA2 SP-SR (Mercer et al. 2012; Fig. 3A); **TSWB.NASP** - CA1 Pyramidal (Zemankovics et al. 2009, Fig. 1B);**TSWB.SLN** - CA3 Pyramidal (Hemond et al. 2008, Fig. 4); **D.NASP** – DG Neurogliaform (Armstrong et al. 2011, Fig.3A, top trace); **D.PSTUT** - CA2 Basket (Mercer et al. 2007, Fig. 5B)**; D.PSWB -** cultured *rutabaga* mutant giant neuron of *Drosophila* (Zhao and Wu 1997, Fig.7, *top left*); **D.ASP.SLN -** neuron in external lateral subnucleus of lateral parabrachial nucleus (Hayward and Felder 1999, Fig.3A, top); **D.RASP.NASP** - CA3 LMR-Targeting (Ascoli et al. 2009, Fig. 1A); **D.TSUT.SLN** - striatal fast-spiking neuron (Sciamanna and Wilson 2011, Fig. 1C); **D.TSWB.NASP** - CA1 Axo-Axonic (Buhl et al. 1994, Fig. 5D). **Abbreviations:** Lat. – lateral; nucl. – nucleus.

Illustrations and Tables

1169 **Table 1.** Representative examples of artificial cerebrospinal fluids

NaCl (mM)	KCl (mM)	$CaCl_2$ (mM)	NaH_2PO_4 (mM)	KH_2PO_4 (mM)	$MgCl_2$ (mM)	$MgSO_4$ (mM)	$NaHCO_3$ (mM)	Glucose (mM)	t (° C)	Pct.	Sample Reference
126	3	2	1.25			2	26	10	34	30.0 %	Canto and Witter, 2012a
124	3.3	2.5		1.2		1	25.5	15	34-35	11.3 %	Ali and Thomson, 1998
120	3.3	1.8	1.23			1.2	25	10	32-34	6.9%	Mott et al, 1997
130	3.5	2.5	1.25		1.5		24	10	32-34	6.5%	Tricoire et al, 2011
126	2.5	2	1.25		2		26	10	34-37	6.5%	Zemankovics et al., 2010
126	3	2	1.25			2	24	10	34-35	5.3%	Buhl et al., 1994
125	2.5	2	1.25		1		25	25	35-37	4.5%	Lübke et al., 1998
124	5	2	1.25			2	26	10	33-35	2.8%	Hamam et al., 2002
124	3	2.5	1.23			1.2	26	10	30	2.0%	Williams et al., 2007

1170

1171 **Table 2.** Representative examples of solutions for patch pipette and micropipette filling

$KMeSO_4$ (mM)	KAc (mM)	KGlu (mM)	KCl (mM)	NaCl (mM)	$MgCl_2$ (mM)	EGTA (mM)	Mg-ATP (mM)	Na_2-ATP (mM)	GTP/ Na_{1-3}-GTP (mM)	PCr/ Na-PCr (mM)	Biocytin (%)	Lucifer yellow (%)	Pct.	Sample Reference
		110	10				4		0.3	10	0.5		29.1%	Canto and Witter, 2012a
		130	7				2		0.3		0.2-0.4		6.9%	Mott et al, 1997
		150			3	0.5	2		0.3		0.2		6.5%	Tricoire et al, 20115
		126					4		0.3	10	0.5		4.9%	Price et al., 2005
		90	27.4	1.8	1.7	0.05	2		0.4	10	0.03		2.8%	Armstrong et al., 2011
		120	20		2	0.1		2	0.3		0.5		2.0%	Hemond et al., 2008
140				4		0.2	4		0.3	10			2.0%	Williams et al., 2007 *
2000											2		11.3%	Ali and Thomson, 1998 *
1500											2		5.3%	Buhl et al., 1994 *
	1000										3		3.2%	Sik et al., 1995 *
	4000		10									4	2.8%	Lacaille et al., 1987 *

1172

1173 **Table 3.** Principles of classification of firing pattern elements

Firing pattern element	Transient responses	Steady-state responses	Characteristics of responses	Values of parameters
Silence	Delayed (D.)		$Delay > DF\frac{ISI_1 + ISI_2}{2}$	$DF = 2$
		SiLeNce (SLN)	$PFS > SF\frac{ISI_n + ISI_{n-1}}{2}$ $PFS > SF * ISI_{\max}$	$SF = 2$
Spiking	Adapting Spiking (ASP.)		$ISI_1 < ISI_2 < ISI_n$; to compare 2 parameter fit $(Y=a_1X+b_1)$ and 3 parameter fit $(Y=a_1X+b_1;\ Y= b_2)$	$p_{2,1}<0.05$ $p_{3,2}>0.025$ $a_1 > 0.003$
	Rapidly Adapting Spiking (RASP.)		$ISI_1 << ISI_2 << ISI_3$ $Y = a_1X + b_1$ $a_1 > S_{RASP}$	$S_{RASP} = 0.2$

			Non-Adapting Spiking (NASP)	$ISI_1 \approx ISI_2 \ldots \approx ISI_n$; to compare 1 parameter fit $(Y=b_1)$ and 2 parameter fit $(Y=a_1X+b_1)$	$p_{2,1}$>0.05
Interrupted	Stuttering	Transient STUTering (TSTUT.)		$ISI_i > F_{pre} * ISI_{i-1}$ $ISI_i > F_{post} * ISI_{i+1}$ $\frac{\sum_{j=i}^{n} ISI_j}{n-j} > F_{pre} \frac{\sum_{j=1}^{i-1} ISI_j}{j}$ (T1.1) $\forall j < i-1: \frac{1}{ISI_j} > f_{\min}$	F_{pre}=2.5 F_{post}=1.5 $f_{\min}$= 25 Hz i=2,3,4
			Persistent STUTering (PSTUT)	$\frac{ISI_i^{\max}}{ISI_{i-1}} + \frac{ISI_i^{\max}}{ISI_{i+1}} > F_{PSTUT}$	F_{PSTUT}=5
	Slow-Wave Bursting	Transient Slow-Wave Bursting (TSWB.)		Inequalities T1.1, $SWA > SWA_{\min}$	F_{pre}=2.5 F_{post}=1.5 $f_{\min}$=25 Hz i=2,3,4 $SWA_{\min}$=5 mV
			Persistent Slow-Wave	$\frac{ISI_i^{\max}}{ISI_{i-1}} + \frac{ISI_i^{\max}}{ISI_{i+1}} > F_{PSWB}$	F_{PSWB}=5 $SWA_{\min}$=5 mV

			Bursting (PSWB)	$SWA > SWA_{min}$	

1194 **Table 4.** Occurrences of completed firing patterns in hippocampal and other neurons

			Steady States			
			NASP	**PSTUT**	**PSWB**	**SLN**
	-	-	**NASP** DG HICAP	**PSTUT** CA1 Neurogliaform	**PSWB** CA3 Pyramidal	—
Transients	-	ASP	**ASP.NASP** CA3 Basket-CCK	**ASP.PSTUT**	**ASP.PSWB**	**ASP.SLN** EC MEC LV Pyramidal
	-	RASP	**RASP.NASP** EC LV Deep Pyramidal	**RASP.PSTUT**	**RASP.PSWB**	**RASP.SLN** CA1 Radiatum Giant
	-	TSTUT	**TSTUT.NASP** EC LV Deep Pyramidal	**TSTUT.PSTUT**	**TSTUT.PSWB**	**TSTUT.SLN** CA2 SP-SR
	-	TSWB	**TSWB.NASP** CA1 Pyramidal	**TSWB.PSTUT**	**TSWB.PSWB**	**TSWB.SLN** CA3 Pyramidal
	D	-	**D.NASP** DG Neurogliaform	**D.PSTUT** CA1 Bistratified	**D.PSWB** *Drosophila* giant	—
	D	ASP	**D.ASP.NASP**	**D.ASP.PSTUT**	**D.ASP.PSWB**	**D.ASP.SLN** Lat. parabrachial nucl.
	D	RASP	**D.RASP.NASP** CA3 LMR-Targeting	**D.RASP.PSTUT**	**D.RASP.PSWB**	**D.RASP.SLN**
	D	TSTUT	**D.TSTUT.NASP**	**D.TSTUT.PSTUT**	**D.TSTUT.PSWB**	**D.TSTUT.SLN** Striatal fast-spiking
	D	TSWB	**D.TSWB.NASP** CA1 Axo-Axonic	**D.TSWB.PSTUT**	**D.TSWB.PSWB**	**D.TSWB.SLN**

1195

NASP	observed in hippocampal neurons	**TSWB.PSTUT**	improbable
D.PSWB	observed in other neurons	—	impossible (no firing)
D.ASP.NASP	not found but possible		

Box 1. Examples of statistically significant correlations between firing patterns and known molecular, morphological and electrophysiological properties in hippocampal neurons

1) None of the 35 **glutamatergic** neuron types show persistent stuttering (**PSTUT**) (p=0.0083). Moreover, none of the neurons with high input resistance ($\mathbf{R_{in}}$) display this steady state (p=0.0478). Thus, all PSTUT cells are GABAergic interneurons with low or intermediate input resistance.
2) Neither any of the 63 **non-projecting** (local circuit) neurons nor any of the 55 **GABAergic** neuron types display transient slow-wave bursting (**TSWB**.) (p=0.0214 and p=0.0215, respectively). Moreover, no neuron type or subtype is found with both TSWB firing and high values of hyperpolarization-induced **sag** potential (p=0.035). In other words, TSWB cells in the hippocampus are a subset of projecting (long-range) glutamatergic neurons with medium or low sags.
3) None of the 15 neuron types that express neuropeptide Y (**NPY**) become silent (**SLN**) after short firing discharge (p=0.0037). In contrast, half of the 14 NPY-negative cells demonstrate this steady state.
4) All of the 10 neuron types that express cholecystokinin (**CCK**) and the overwhelming majority of neuron types with high input resistance (17/18) display adapting spiking (**ASP.**) (p=0.0113). In contrast, this transient state is observed in just above half of CCK-negative cells (9/16) and two-thirds of cells with low or intermediate $\mathbf{R_{in}}$ (12/18).

5) Of 14 neuron type with **wide AP**, only one (EC LV-VI Pyramidal-Polymorphic) shows delayed (**D.**) firing (p=0.021). In contrast, nearly half of neuron types without wide AP demonstrate this transient state.
6) With the exceptions of DG Semilunar Granule and CA1 O-LMR, none of the neurons with high threshold potential ($\mathbf{V_{thresh}}$) display transient stuttering (**TSTUT.**) (p=0.0481); similarly, none of the neurons with high amplitude of fast afterhyperpolarization (**fAHP**), except CA1 Cajal-Retzius, demonstrate TSTUT. (p=0.0098).

The p values are computed using Bernard's exact test for 2×2 contingency tables (see *Materials and Methods*).

1199

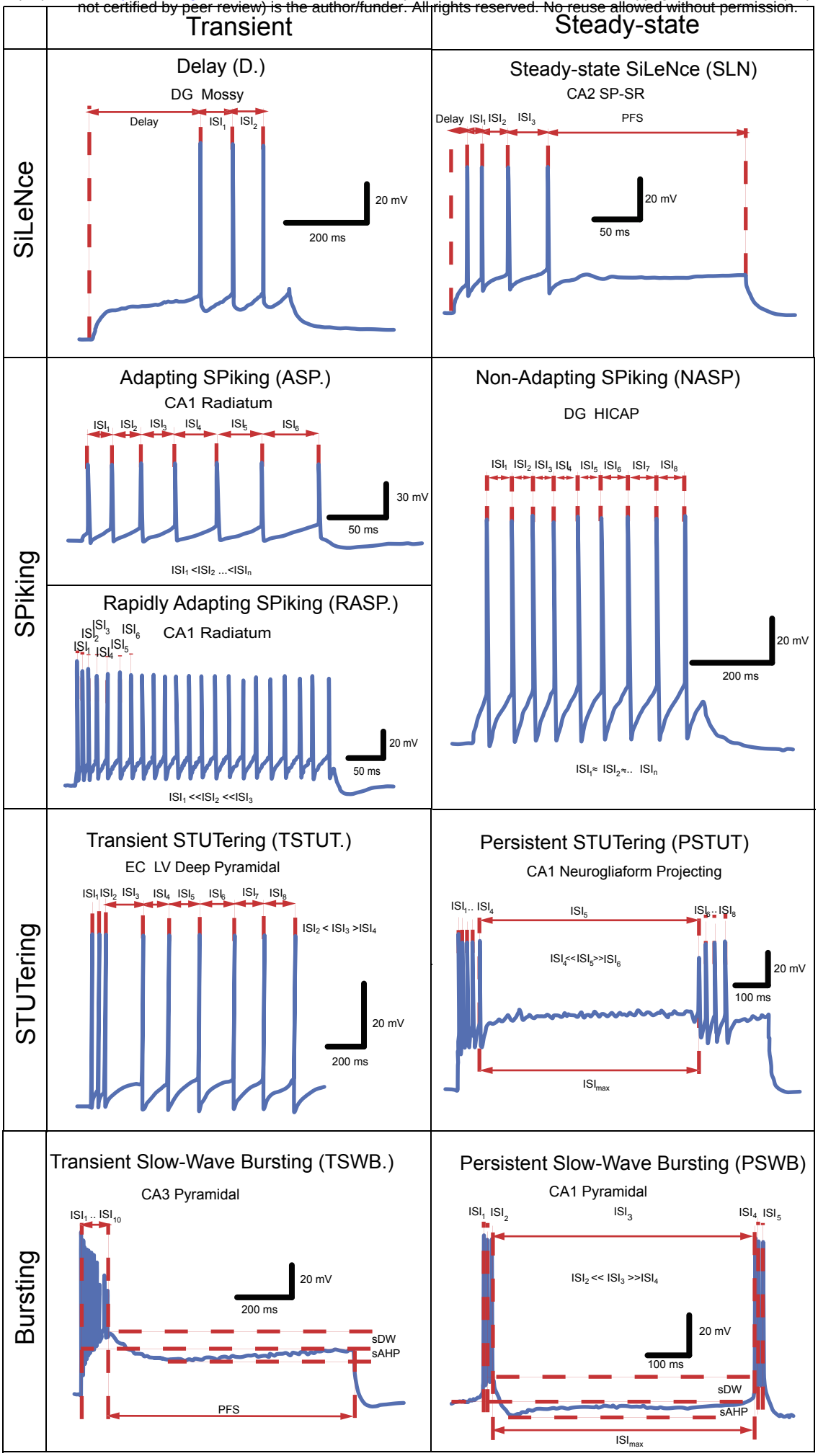

Figure 1

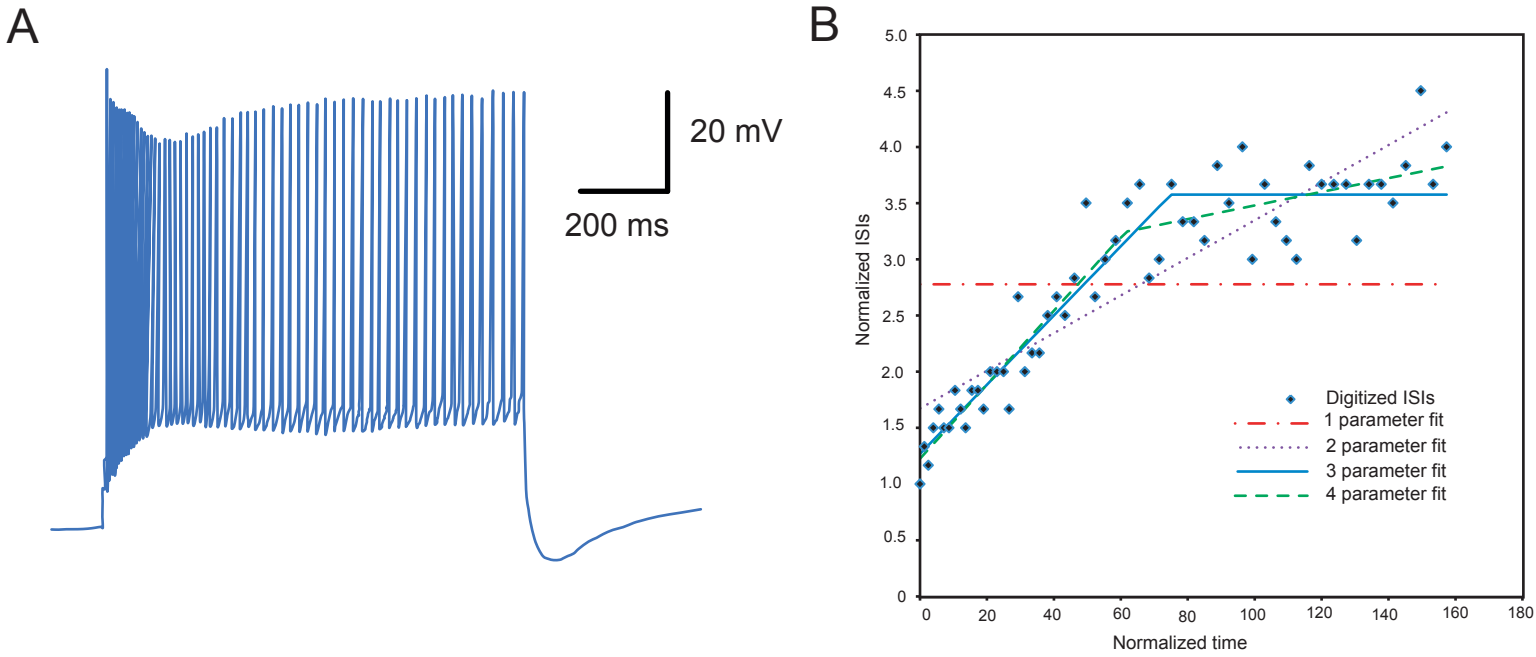

Figure 2

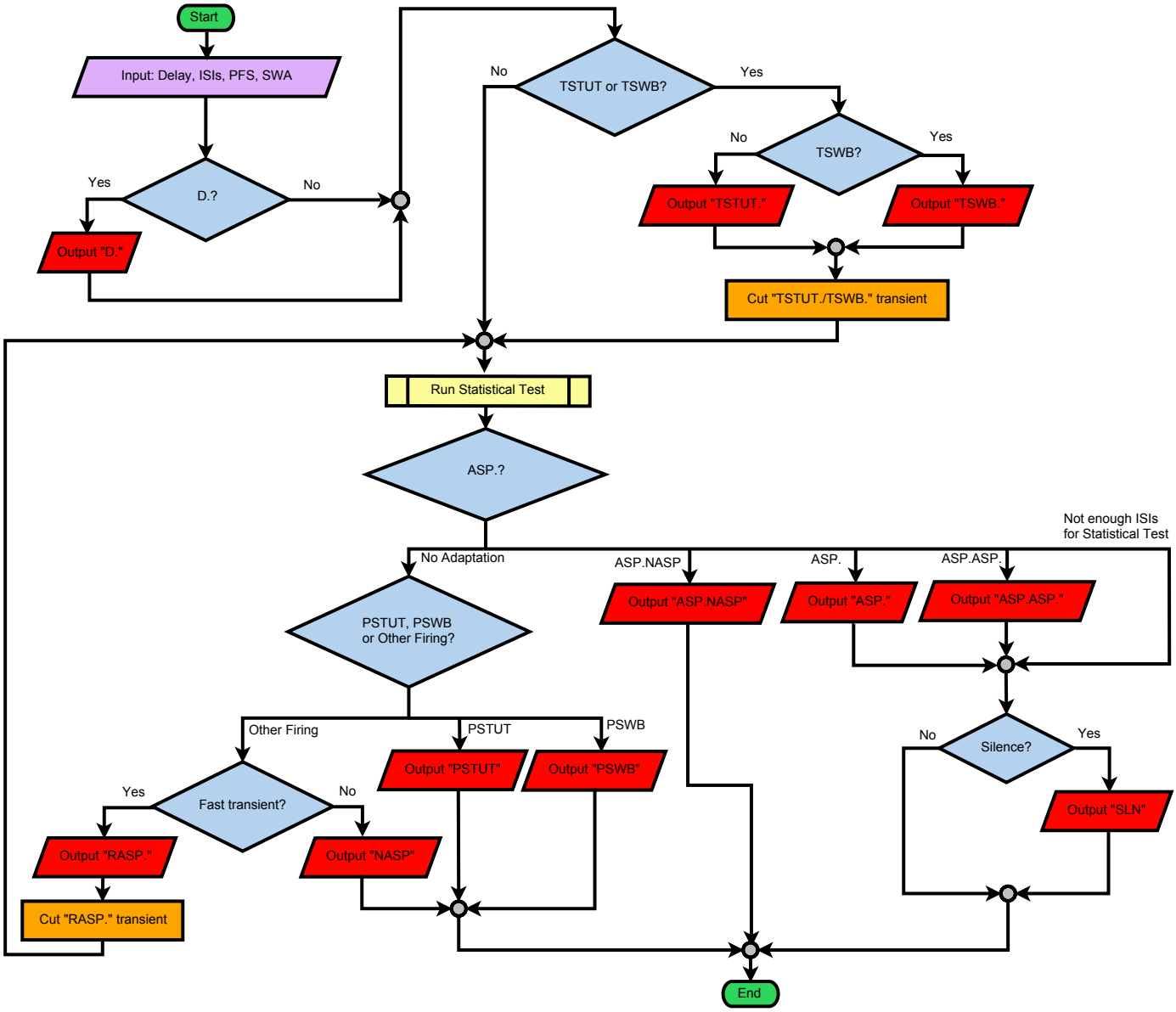

Figure 3

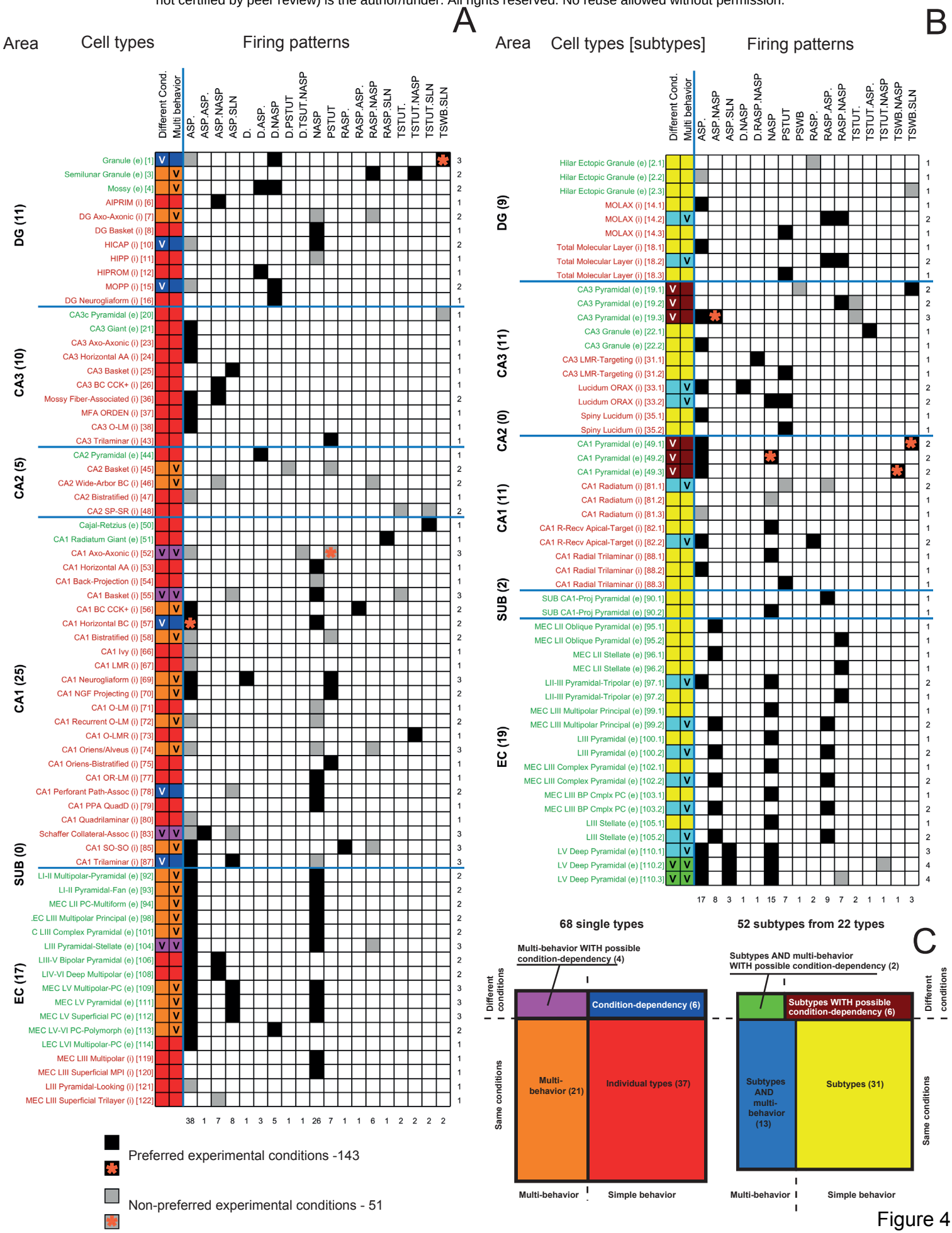

Figure 4

A

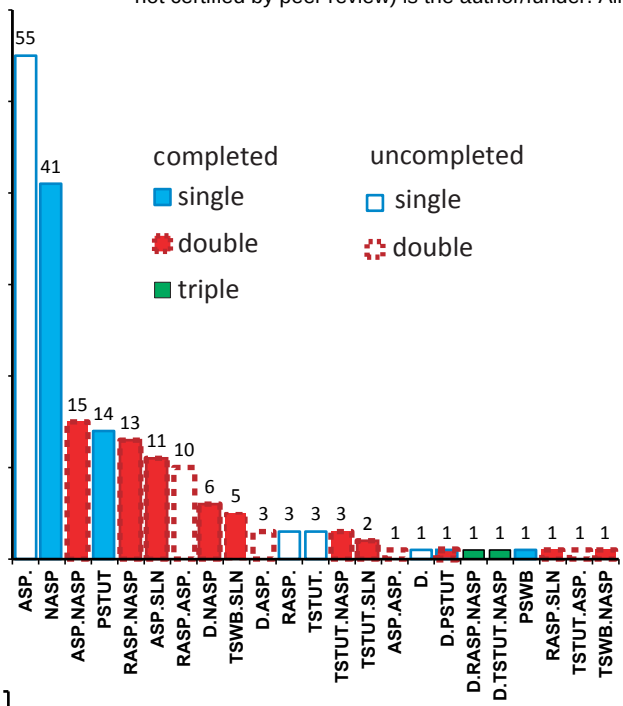

B

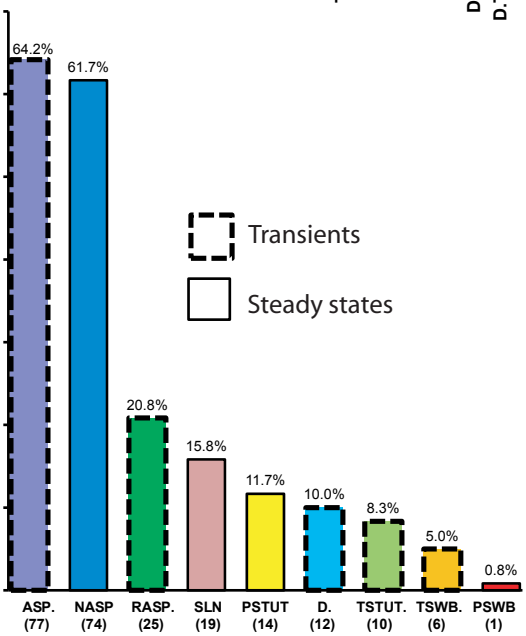

C

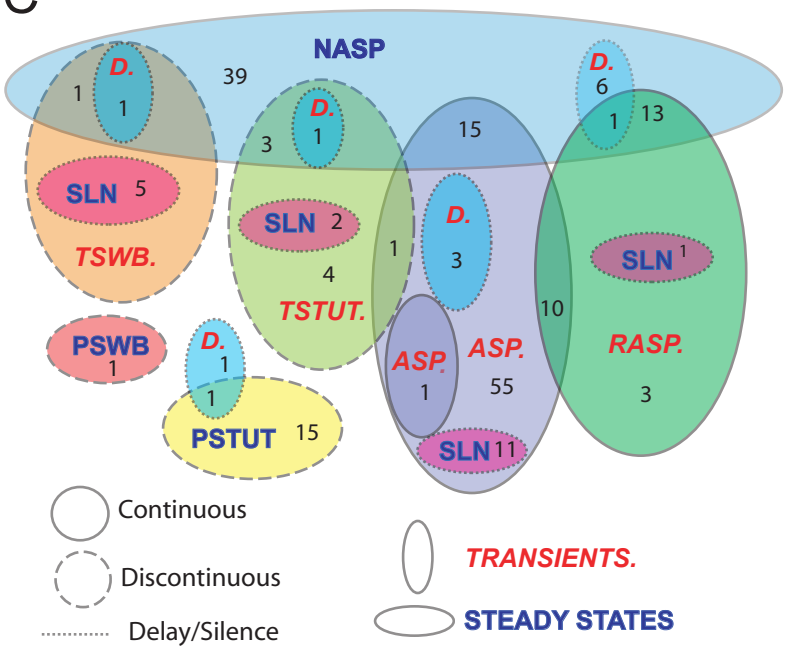

Figure 5

A

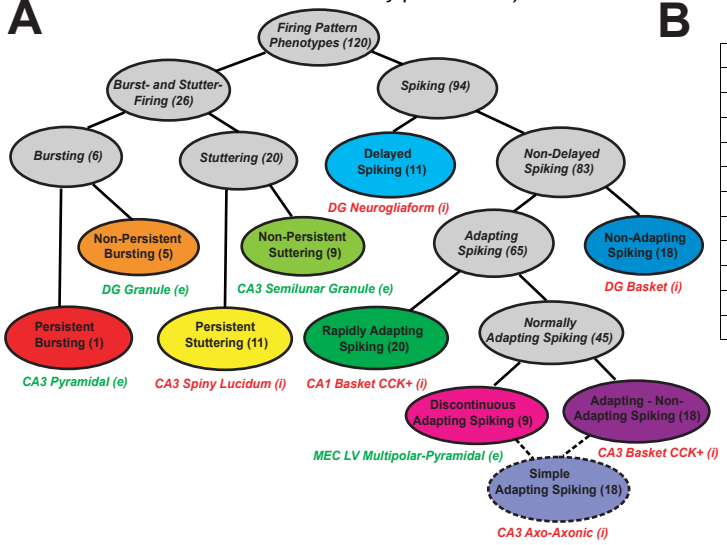

B

	Firing Pattern Elements								
Firing Pattern Phenotype Family	ASP.	D.	NASP	PSTUT	PSWB	RASP.	SLN	TSTUT.	TSWB.
Persistent Bursting (1)	0%	0%	0%	0%	100%	0%	100%	0%	100%
Non-Persistent Bursting (5)	60%	20%	40%	0%	0%	0%	80%	0%	100%
Persistent Stuttering (11)	27%	0%	9%	100%	0%	9%	0%	0%	0%
Non-Persistent Stuttering (9)	44%	0%	67%	0%	0%	22%	44%	100%	0%
Delayed Spiking (11)	73%	100%	64%	27%	0%	9%	0%	9%	0%
Non-Adapting Spiking (18)	0%	0%	100%	0%	0%	0%	0%	0%	0%
Simple Adapting Spiking (18)	100%	0%	0%	0%	0%	0%	0%	0%	0%
Discontinuous Adapting Spiking (9)	100%	0%	78%	0%	0%	11%	100%	0%	0%
Adapting - Non-Adapting Spiking (18)	100%	0%	100%	0%	0%	0%	0%	0%	0%
Rapidly Adapting Spiking (20)	70%	0%	75%	0%	0%	100%	5%	0%	0%

C

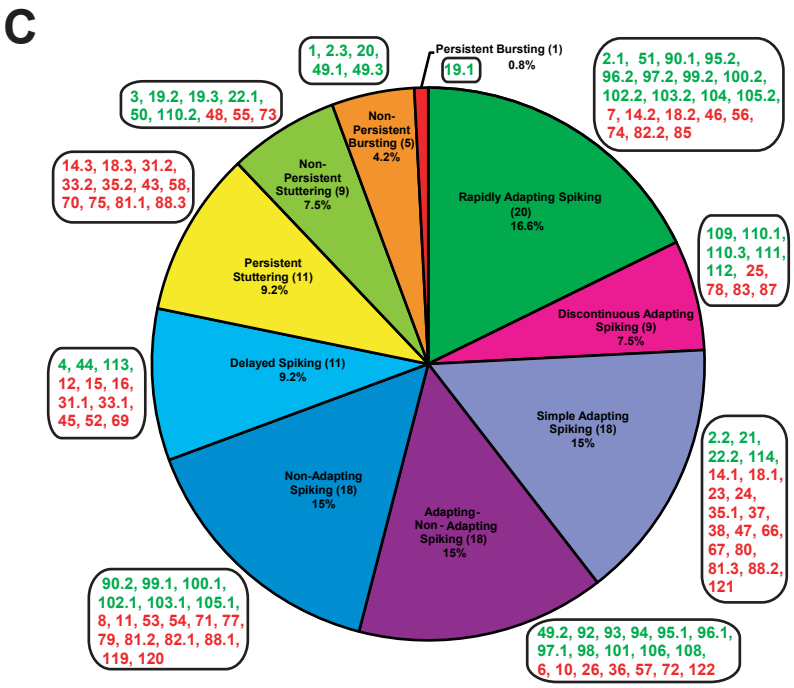

D

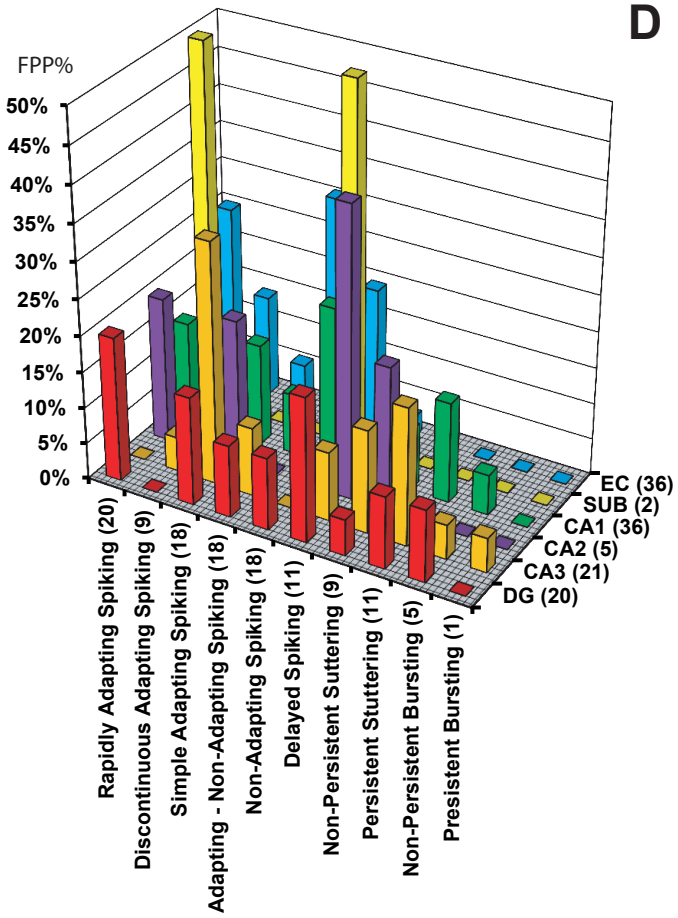

Figure 6

A. Search by Property

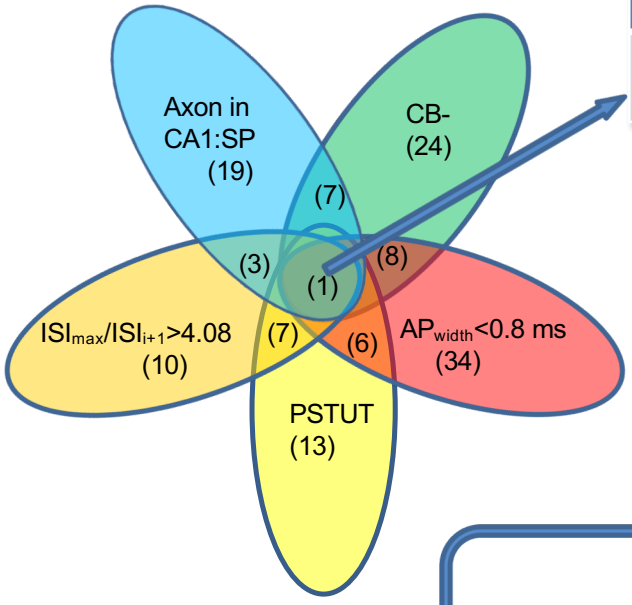

B. Neuron Page

Neuron Type

CA1 Axo-Axonic

C. Firing Pattern Evidence Page

CA1 Axo-Axonic

Firing pattern: persistent stuttering (PSTUT)

Source: Pawelzik H, Hughes DI, Thomson AM. Physiological and morphological diversity of immunocytochemically defined parvalbumin- and cholecystokinin-positive interneurones in CA1 of the adult rat hippocampus. J Comp Neurol (2002) 443 (4), 346 – 367. PMID: 11807843

Page location: p. 353, Fig. 4B, bottom

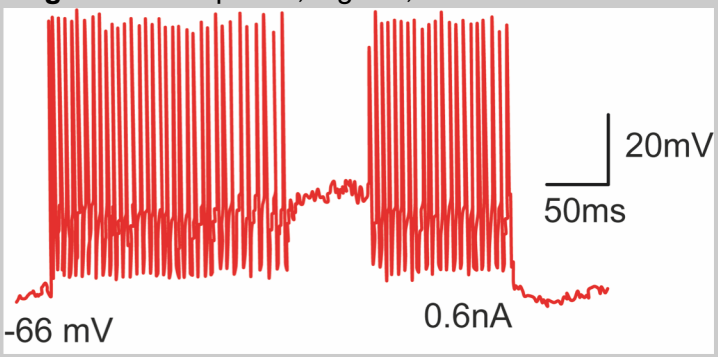

Parameters: Tstim = 356 ms, Istim = 600 pA

Author original FP description: interrupted fast-spiking discharge pattern

Linking PMID: 11807843

Linking Quote: All necessary morphological evidence is present in this self-same publication.

D. Firing Pattern Parameters

Parameter Name	Value
Delay [Latency of first spike]	0.02 ms
PFS [Post Firing Silence]	8.45 ms
NISI [Number of ISIs]	53
ISI_{AV} [Average ISI]	6.59 ms
Max ISI [Maximum Interspike Interval]	67.03 ms
Min ISI [Minimum Interspike Interval]	2.85 ms
MaxISI/MinISI [Maximum ISI ratio]	23.55
MaxISIn /ISI_{n-1} [Ratio MaxISI to the previous ISI]	9.78
MaxISIn /ISI_{n+1} [Ratio MaxISI to the next ISI]	13.74
. . .	. . .

E. Animals

Parameter	Value/ Characteristic
Species	rats
Inbred strain	Dawley Sprague
Age/Postnatal days	adult
Sex	male
Weight (g)	120-200
. . .	. . .

H. Solution

ACSF Parameter	Value
NaCl (mM)	124
KCl (mM)	3.3
$CaCl_2$ (mM)	2.5
KH_2PO_4 (mM)	1.2
$MgSO_4$ (mM)	1
$NaHCO_3$ (mM)	25.5
Glucose (mM)	15
O_2 %	95
CO_2 %	5
t (°C)	34-36
. . .	. . .

I. Interspike Intervals

F. Preparation

Parameter	Value / Characteristic
Type of preparation	slice
Orientation	coronal
Thickness (μm)	450
. . .	. . .

G. Recording

Parameter	Value / Characteristic
Method	Intracellular recording
$KMeSO_4$ (mM)	2000
Biocytin (%)	2
. . .	. . .

Figure 7

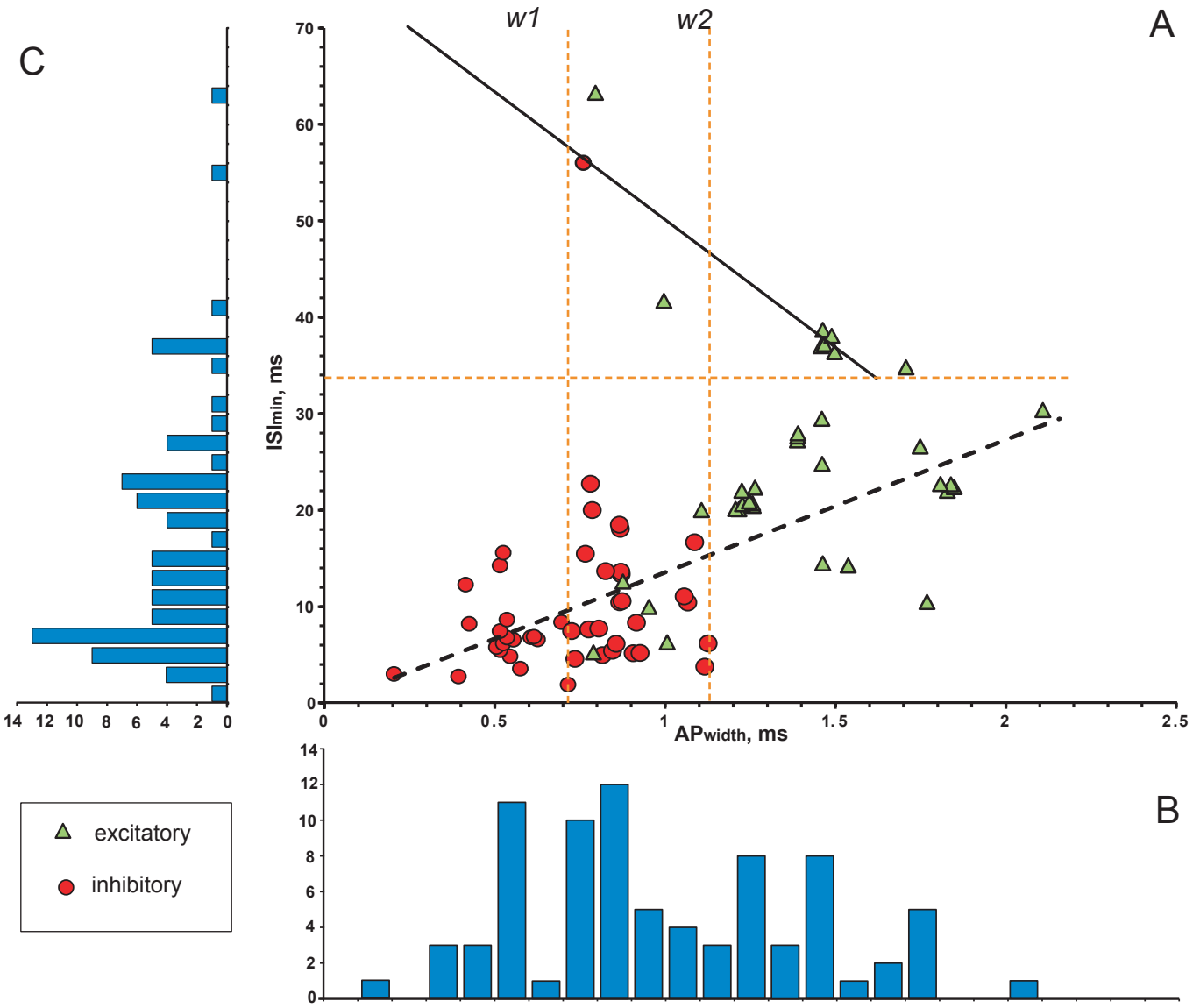

Figure 8